CHALMERS
UNIVERSITY OF TECHNOLOGY

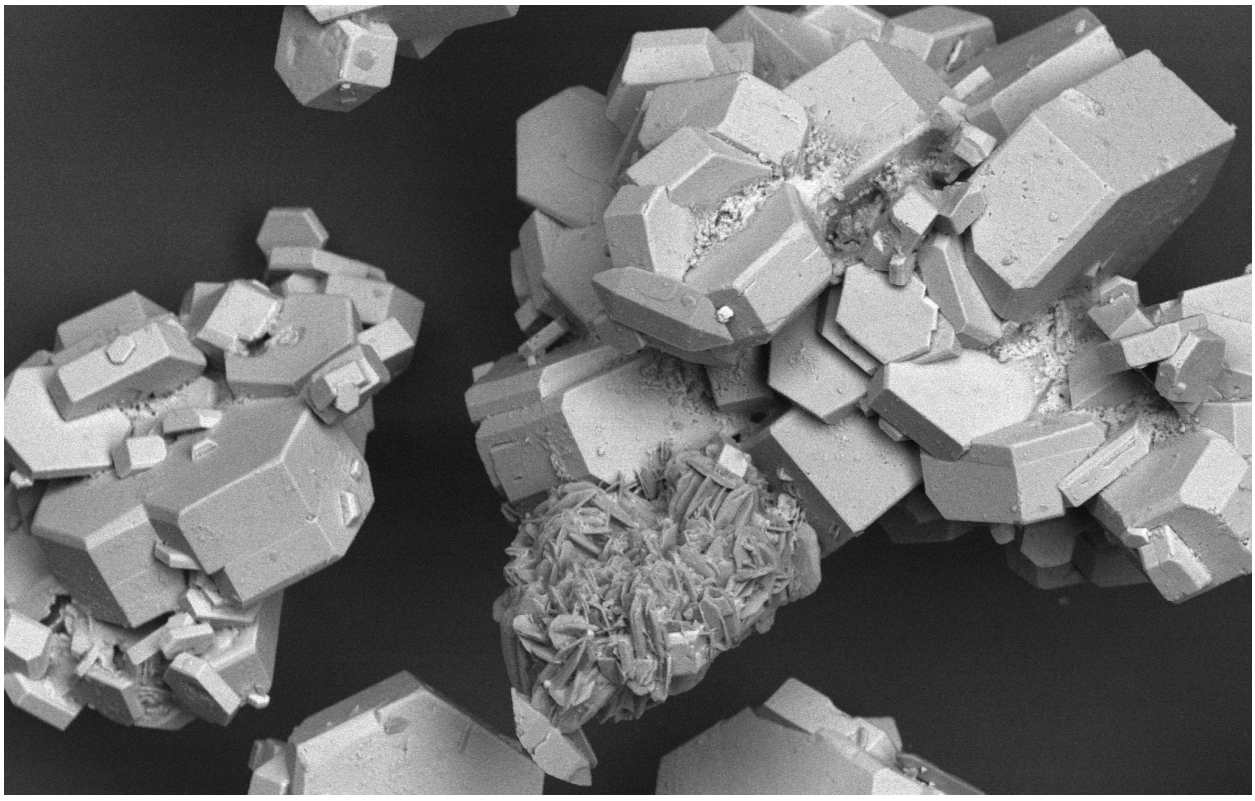

Potassium Recovery from Purge Streams in Pulp Mills

Process Development and Evaluation

Master's thesis in Sustainable Energy Systems

OLIVIA LUNDBORG
JENNY REGNSTRAND

DEPARTMENT OF CHEMISTRY AND CHEMICAL ENGINEERING
CHALMERS UNIVERSITY OF TECHNOLOGY
Gothenburg, Sweden 2025
www.chalmers.se

Master's thesis 2025

Potassium Recovery from Purge Streams in Pulp Mills

Process Development and Evaluation

Olivia Lundborg, Jenny Regnstrand

CHALMERS
UNIVERSITY OF TECHNOLOGY

Department of Chemistry and Chemical Engineering
Division of Applied Chemistry
Chalmers University of Technology
Gothenburg, Sweden 2025

Potassium Recovery from Purge Streams in Pulp Mills
Process Development and Evaluation
OLIVIA LUNDBORG
JENNY REGNSTRAND

Supervisor: Liubov Vasenko, Valmet
Examiner: Diana Bernin, Department of Chemistry and Chemical Engineering

Master's Thesis 2025
Department of Chemistry and Chemical Engineering
Division of Applied Chemistry
Chalmers University of Technology
SE-412 96 Gothenburg
Telephone +46 31 772 1000

Cover: Image of the intermediate product, obtained during run 1.7 at 15 °C. The image was taken by Emmanouela Leventaki.

Typeset in LaTeX
Printed by Chalmers Reproservice
Gothenburg, Sweden 2025

Potassium Recovery from Purge Streams in Pulp Mills
Process Development and Evaluation
OLIVIA LUNDBORG, JENNY REGNSTRAND
Department of Chemistry and Chemical Engineering
Chalmers University of Technology

Abstract

In pulp mills, non-process elements such as potassium and chloride accumulate over time and must be discarded through a purge stream to maintain process efficiency and prevent equipment degradation. Currently, the purge stream is directed to effluent treatment. It contains valuable material that could be recovered, but such a process is not implemented today. The aim of the project was to evaluate and develop a new process for recovering potassium from the purge streams of two different mills. The potassium is converted into a commercial product via an intermediate, and can be used as a fertilizer. This new process was compared to the conventional production of the commercial product, in terms of energy demand and process design. The project began with a literature study, followed by an experimental phase focused on cooling crystallization of the intermediate and re-crystallization of the final product. Analytical methods used were ICP-AES, XRD, SEM-EDX and dry solids analysis, to determine elemental composition and dry solid content. MATLAB was used as a simulation tool to estimate the energy demand of the cooling crystallization. The process of recovering the intermediate was found to be sensitive and highly dependent on the composition of the purge stream. The highest purity of the intermediate product was found at 15 °C with slow cooling of the purge stream from Mill 2. The re-crystallization to the commercial product was most effective with a leaching solution containing 50/50 wt% ML2 mimic and saturated solution of potassium chloride for both mills. The new process was shown to have a lower energy demand than the conventional process, especially with slow cooling applied. Further, it was proved to be safer with respect to by-products and operational parameters. In conclusion, the new process shows potential in recovering potassium, contributing to the pulp mills circular economy and sustainability. Nonetheless, further optimization of process conditions and an economic assessment are necessary to validate its industrial viability.

Keywords: cooling crystallization, re-crystallization, ash treatment, pulp mill, process circularity

Acknowledgements

This thesis was written at Valmet within the Ash Treatment Group.

We would like to sincerely thank Valmet for their support and collaboration throughout this project. We are also grateful to Emmanouela Leventaki for her valuable assistance with the solid analysis and for taking all the SEM-EDX images. Finally, we are especially grateful to our supervisor, Liubov Vasenko, for her guidance and expertise.

O. Lundborg & J. Regnstrand, Gothenburg, May 2025

List of Acronyms

Below is the list of acronyms that have been used throughout this thesis, listed in alphabetical order:

DS	Dry Solid
IAP	Ion Activity Product
ICP-AES	Inductively Coupled Plasma Atomic Emission Spectroscopy
ML1	Mother Liquor 1
ML2	Mother Liquor 2
NPE	Non-Process Elements
SI	Saturation Index
SEM-EDX	Scanning Electron Microscopy with Energy-Dispersive X-Ray Spectroscopy
XRD	X-Ray Diffraction

Nomenclature

Below is the nomenclature of indexes, prefixes, parameters, terminology and variables that have been used throughout this thesis.

Indexes

j	Index for jacket
P	Index for powder
$reactor$	Index for bleed stream in reactor

Prefixes

S	Prefix for cans containing bleed stream from Mill 1
F	Prefix for cans containing bleed stream from Mill 2

Parameters

Cp_j	Specific heat capacity of the medium in the jacket
ρ_j	Density of the medium in the jacket
$\mathrm{m}_{reactor}$	Mass of bleed stream in reactor

Terminology

Product A	Intermediate double-salt of potassium and sodium
Product B	Commercial potassium salt
Product C	Competing phase

Variables

$\dot{m}_{cooling}$	Mass flow of cooling medium in jacket
$\mathrm{T}_{j,inlet}$	Jacket inlet temperature
$\mathrm{T}_{j,outlet}$	Jacket outlet temperature
$\mathrm{T}_{reactor}$	Temperature of bleed stream in reactor
$\dot{Q}_j$	Heat transfer between the cooling medium and reactor

Contents

List of Figures

List of Tables

1
Introduction

This chapter gives an introduction to the project and the reason behind the research. It will present a valuable background, the aim of the project and relevance of the research, as well as the structure of the thesis.

1.1 Background

The importance of a social adjustment is crucial, and sustainability plays a big role in addressing climate change by reducing emissions, promoting resource efficiency, and ensuring long-term balance [1]. The reliance on fossil fuels and non-renewable resources are a few of the most pressing challenges that must be solved. One solution is to utilize more renewable resources, such as lignocellulosic materials. By doing this, waste from forestry can be valorized and impacts from end-of-life treatment, such as pollution, can be avoided. It improves the circularity and helps with minimizing the loss of material. Over the past few years, biorefineries have been developed to utilize as much of the biomass as possible, and new processes have been integrated. This has made biorefineries more competitive and economically feasible, which is important for their survival [1].

A way to make biorefineries more sustainable, is to take care of the waste and emissions in an efficient way [2]. Examples of waste from a biorefineries are ash, wastewater and residues from the chemical treatment. Taking advantage of potential waste through methods that manage or convert it into valuable products, while simultaneously reducing the need for disposal, is an economically favorable approach [2].

1.1.1 Kraft Pulp Mills

A pulp mill is a biorefinery where the biomass is usually wood, and the products are mass, pulp, fibers, and fuel [3]. The purpose of pulping is to process wood and separate cellulose fibers from lignin and hemicellulose. Cellulose can then be used to make pulp or dissolved pulp, which is further utilized to produce several commercial products. The decomposition and treatment of wood can be done in an alkaline or acid environment. This report will focus on the first, which is called Kraft pulping, where the cooking chemical is sodium hydroxide [3].

During the pulping process a solution called black liquor is formed, which contains

lignin, cooking chemicals, and other residues [4]. The black liquor is concentrated in an evaporator where water is removed, and then it is burned in a recovery boiler where energy is generated. During combustion, the cooking chemicals are recovered and transported back into the process [4]. A schematic representation of a Kraft pulp mill is shown in Figure 1.1.

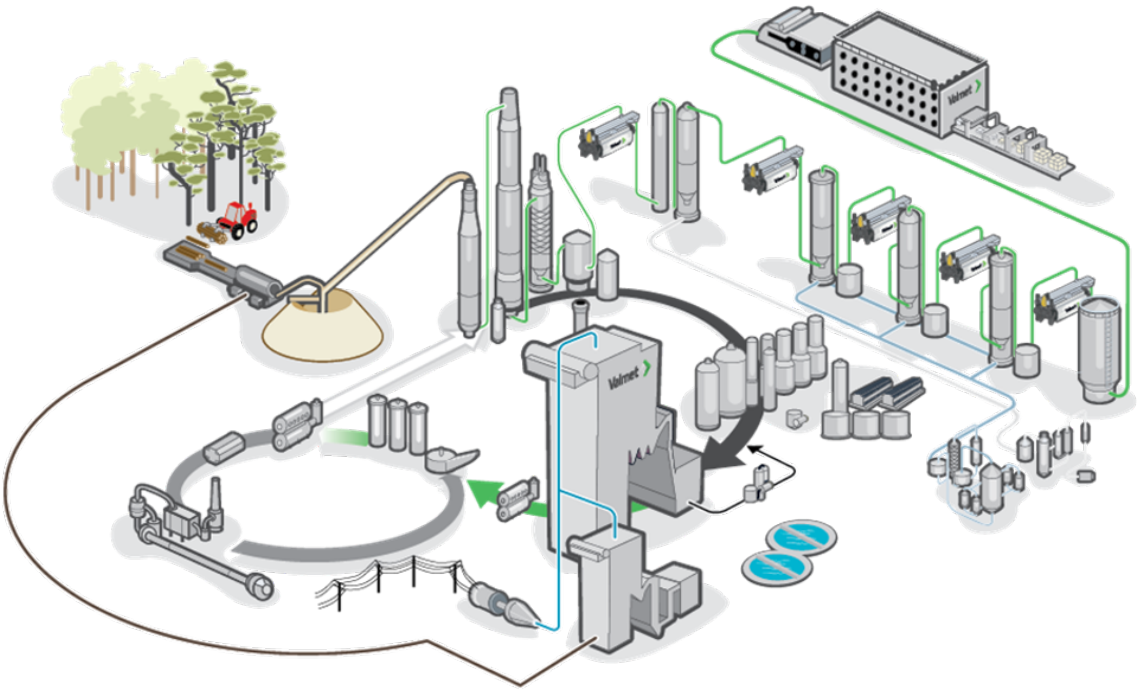

Figure 1.1: *A schematic over a Kraft pulp mill (reproduced from Valmet, 2024, with permission).*

1.1.2 Ash Treatment Technology

The flue gases that are leaving the recovery boiler contain ash. This ash is recovered in order to increase the circularity of the entire process. A more circular process decreases the use of additional chemicals and energy, which improves the environmental impact. Since some chemicals in the ash can be harmful, the environmental impact is further improved by not releasing them into the atmosphere. If an ash treatment technology is implemented, useful chemicals found in the ash can be recirculated back to the mill while unwanted chemicals hold the potential to be sold as commercial products.

The unwanted chemicals mainly consist of potassium and chloride and will be referred to as non-process elements, NPEs. These chemicals can enter the mill with wood, water and make-up chemicals [5]. If these are not removed, they can cause damage to the equipment and make the process less efficient. NPEs will for example lower the melting temperature of the ash, which entails that it will become sticky at lower temperatures [6]. If the ash is sticky, there will be a higher risk for fouling and an increased consumption of blowing steam and wash water in the boiler. Recirculating NPEs in the black liquor will also cause an increased risk for corrosion in

the equipment, and consequently an increased need for maintenance. Furthermore, NPEs reduce the calorific value of black liquor, thus a greater volume is required to generate the same amount of energy.

To remove excess NPEs and keep their concentration stable in the mill streams, a stream, mostly containing NPEs, is purged during ash treatment and sent to effluent treatment. This stream is referred to as a bleed stream. In order to increase the circularity of the process further, there is an interest in recovering the NPEs, instead of bleeding them out.

1.2 Statement of the Problem

The current process does not utilize or recover any chemicals from the bleed stream, even though it contains a lot of valuable material. This study evaluates the recovery process of potassium, an NPE, from the bleed stream and its conversion into a commercially viable salt via the formation of an intermediate. Additionally, parameters influencing the efficiency of the process will be defined and the physical and chemical properties of various process streams will be examined.

Today, there is a limited data availability on the feasibility of potassium recovery from the bleed stream. In 2023 and 2022, Valmet conducted internal experiments with bleed streams from two mills, which will be presented in Section 2.2.3.1 and 2.2.3.2 respectively. The results from one of these experiments indicated that there may be a possibility of recovering potassium, through the intended method. However, no other investigation has been made until now by Valmet. The mills evaluated in this report are the same as in the previous experiments.

1.3 Aim and Objectives

The overall objective is to enhance circularity by recovering more chemicals for a greater economic and environmental sustainability. The aim of the project is to evaluate the process of recovering an intermediate potassium salt from the bleed stream, and to investigate methods for converting it into a commercial product. During the project, parameters that impact the efficiency of the process will be defined and evaluated. The physical and chemical properties of different process streams will be analyzed and determined. The investigated process will be compared to a conventional production of the commercial product in terms of energy demand.

1.4 Research Relevance

The research will help in the development of ash treatment and recovery of chemicals from pulp mills. As mentioned, NPEs are usually discarded, this will however not be sustainable in a long-term perspective. Increasing circularity will always be of great relevance for a big industry. There can be a lot of drivers for this, the most

relevant might be compliance with regulation, pressure from customers, improving firm and brand image and economical drivers [7]. If a process for recovering, otherwise discarded, chemicals and transforming them into commercial products would be implemented, there would be increased incomes and potentially other economic incentives. The company can also be seen as more proactive. As of today, regulations regarding what is allowed for industries to send to effluent treatment is getting stricter in many countries and are further developed by the European Commission [8]. Therefore, it is profitable to be investigating the possibility of recovering chemicals from effluent streams as it will benefit the company economically and the overall environment.

Furthermore, the commercial potassium salt is commonly used as a fertilizer, which can be of interest for the pulping industry. Logging is an act within forestry management, where trees are cut and removed from the forest and serve as the main feedstock for pulp production. All management activities in the forest will impact the nutrient balance [9]. Nutrients that support plant growth can be lost through leaching and run-off after such activities, which would have a negative impact on the sites near-term regeneration. However, since the commercial product can be used as a fertilizer, there is a possibility to restore some of the nutrients to the soil and stimulate growth of new trees.

1.5 Overview of Methodology

The project was completed through a literature study and an experimental phase. The purpose of the literature study was to establish a solid foundation for the experiments and give a more comprehensive understanding of the process. Research was done through reading articles, reports and patents with similar investigations and experiments. The experimental process was divided into two steps, where the main methods used were cooling crystallization and re-crystallization. Originally, the experiments were designed as full factorial, with three different factors for each step. Elemental composition and the dry solid content, DS, of liquid and solid samples were analyzed to construct the overall mass balance and determine the efficiency of potassium recovery. Analytical methods that were used were ICP-AES, SEM-EDX, XRD and dry solids analysis.

A more in-depth description of the methodology is presented in Chapter 3.

1.6 Limitations

This study provides valuable information on the potassium recovery process, however, there are several limitations that must be considered. The project will solely focus on the recovery of potassium from the bleed stream. Furthermore, since this project is done in collaboration with Valmet, some information is confidential. The intermediate product will be referred to as Product A, and the commercial product will be referred to as Product B. The chemical formulas or names will not be

disclosed. Furthermore, two bleed streams from different mills will be used in the experimental phase. There is Mill 1, which is in Sweden, and Mill 2, which is in Finland. There will not be a full analysis of the liquid samples, only potassium, sodium and sulfur will be analyzed. Other ionic interactions can therefore not be taken into consideration.

1.7 Structure of the Thesis

Chapter 1 offers a background, to give some perspective and context to the subject that will be discussed in this project. It also includes the motivation for the study and an overview of the method used. Chapter 2 will cover all relevant literature used for the research. In Chapter 3, the methodology for data collection and analyses is described in detail. The results, and a discussion of these will be presented in Chapter 4, while Chapter 5 will consist of the conclusions from the study and suggestions for improvement and further research.

2
Theory

The purpose of this chapter is to present relevant theoretical information to support understanding of the project. It will go through physical and thermodynamic mechanisms, different approaches for potassium recovery from a liquid stream, previously executed experiments and the conventional production of Product B, among others.

2.1 Crystallization, Purification and Solid/Liquid Separation

This section aims to disclose the fundamental mechanisms of crystallization. It is a process to form a solid crystal from a solution through supersaturation. The section also describes solid/liquid separation techniques including filtration, sedimentation, and drying, which are essential for isolating and producing the crystalline product.

2.1.1 Crystallization

The formation of solid crystals from a solution is called crystallization and can be performed through several different processes [10]. When the solubility conditions change, such as lowering the temperature or adjusting the concentration of the solvent, a crystal product can be separated from a liquid stream. Crystallization consists of two major steps, nucleation and crystal growth. During nucleation, the solute molecules that are dispersed in the liquid start to aggregate and become stable. The aggregate creates the nuclei of the crystal. However, under unstable conditions, the nuclei dissolve. To prevent that from happening, the aggregates need to reach a critical size which is decided by the operation conditions. The second part of crystallization is crystal growth, which is the subsequent growth of the nuclei. The driving force of crystallization is supersaturation, and both nucleation and crystal growth occur simultaneously during that condition. Supersaturation can be reached through cooling, anti-solvent addition, evaporation, pH adjustment, or chemical reaction. Depending on the supersaturation degree, either mechanism can be dominant, which will result in different sizes and shapes of the crystals. The saturation index, SI, can indicate if a solution is supersaturated, saturated, or undersaturated for a certain product [11]. This can be calculated according to equation (2.1), where IAP is the ion activity product and K_{sp} is the solubility product constant. For diluted solutions, the IAP can be calculated using molar concentrations as simplification. This can be done according to equation (2.2) for double salts. A higher value of IAP increases the probability of the specific product

to be crystallized from the solution. If SI > 1, the solution is supersaturated, if SI $= 1$, it is saturated, and if SI < 1, it is undersaturated.

$$SI = \log\left(\frac{\text{IAP}}{K_{\text{sp}}}\right) \tag{2.1}$$

$$IAP = [A]^a \cdot [B]^b \cdot [C]^c \tag{2.2}$$

It is desirable to have well-formed crystals since this is usually a sign of purity [10]. When crystals are symmetric, it indicates that the molecules have fit perfectly into the lattice, leaving no room for impurities. However, there can also be crystals where impurities have been incorporated, which decreases the quality of the final product. To prevent impurities in crystals, it is important to control the process. One way is to have a slower crystallization rate by regulating the temperature, as this affects the crystal size and quality. In this project, the main approach to create supersaturation is by lowering the temperature. This is called cooling crystallization. In cooling crystallization, the solubility of the solute is decreased by lowering the temperature of the solution, as most solutes are less soluble at lower temperatures. This leads to supersaturation and crystals begin to form. Gradual and slow crystallization helps the crystals to be well-formed by giving the molecules time to align correctly. This encourages the formation of larger, well-ordered crystals and prevents impurities from attaching.

2.1.2 Re-Crystallization

Re-crystallization is a subset of crystallization and is mainly used to purify crystals [12]. Solids are mixed with a liquid solution with a certain composition and conditions that promote the undesired impurities of the original crystals to be dissolved while keeping the desired product in solid phase. To reduce impurities in the crystals, their solubility in the solvent must be higher than that of the main product. The process may need to be repeated, and there might be some losses of the desired component as well.

2.1.3 Solid/Liquid Separation

To separate the crystals from the liquid, filtration is a common method [10]. The operation is done through a medium where the liquid alone can pass, while the crystals are retained. For high-quality separation, the filtration medium must capture even the smallest crystals, however, fine particles filter poorly as they tend to hold more liquid. A high-quality separation can also be achieved by repeating the filtration more than once. Another way to separate solids from liquid is by sedimentation [13]. The difference between that and filtration is that filtration is mechanical while sedimentation is based on gravity. The driving force is the difference in specific gravity between the phases. This difference can be enhanced by increasing the mass of individual particles. An additional separation technique is centrifugal filtration. It is a mechanical process that separates solids from liquid by applying centrifugal force. This technique is especially useful when solid particles are very fine or difficult

to filter. It is a fast, continuous, and efficient separation process but quite energy demanding for large scale operations. However, the separation is not fully complete after either filtration or sedimentation, as the solid crystals remain wet and may require drying [10]. The removal of liquid, such as water or solvent, by evaporation from a solid is called drying [10]. It is a mass transfer process and is commonly used after filtration. Drying often involves a source of heat to discard the excess liquid, but it can be done in several different ways. However, this project will not focus on drying the final product.

2.2 Recovery of Potassium from the Bleed Stream in a Pulp Mill

As first mentioned in Section 1.1.2, it would be desired to recover the intermediate Product A from the bleed stream in a pulp mill. The goal is to transform this into the commercially viable Product B and enhance the circularity within the mill as well as generate profit. Product B is an inorganic crystalline salt of potassium which is primarily used as a fertilizer [14]. It is particularly used for crops that are sensitive to chloride ions, helping them to absorb a higher amount of readily available nutrients. Furthermore, Product B has industrial value, for example, when manufacturing glass. To achieve the desired recovery, a two-step reaction should be performed due to thermodynamic constraints [15].

2.2.1 Step 1: Cooling Crystallization of Intermediate Product A

The first step of the recovery is crystallization, where Product A is formed. The unbalanced, conventional, reaction can be seen in equation (2.3) [16]. During the reaction Product A, which is a double salt of sodium and potassium, is formed as a solid in an aqueous solution of sodium chloride.

$$Na_2SO4\ (aq) + KCl\ (s) \xrightarrow[Cooling]{} Product\ A\ (s) + NaCl\ (aq) \tag{2.3}$$

The bleed stream that will be used during the experimental phase contains potassium, chloride, sodium, sulfate and carbonate ions. Thus, reactants seen in equation (2.3), are found in the bleed stream. In addition to Product A, a mother liquor is produced during the reaction, this is the remaining liquid phase after crystallization. The mother liquor produced when using the bleed stream as a reactant is an aqueous salt solution. The modified reaction can be seen in equation (2.4).

$$Bleed \xrightarrow[Cooling]{} Product\ A\ (s) + Mother\ Liquor\ 1\ (aq) \tag{2.4}$$

There are multiple suggestions regarding the appropriate temperature for performing the reaction. It is implied that it can be conducted at ranges between 5-50 °C [15]. However, it is more commonly suggested to use a more moderate temperature, generally closer to room temperature [15][16][17][18]. Furthermore, in one example the process was carried out under vacuum at a temperature of 40–45 °C [19]. The

bleed stream is at approximately 80-100 °C when it is rejected from the process, therefore supplementary cooling is suitable for crystallization in the first step. Figure 2.1 shows how the concentration of dissolved ions in a bleed stream is altered according to temperature. The analysis of the bleed stream from Mill 1, conducted during the 2023 experiment, was used to create this figure. It can be used to determine the most appropriate target temperature for the first step. For example, at approximately 25 °C there is a minimum concentration of dissolved potassium ions. The potential maximum recovery of potassium should therefore be possible at this temperature.

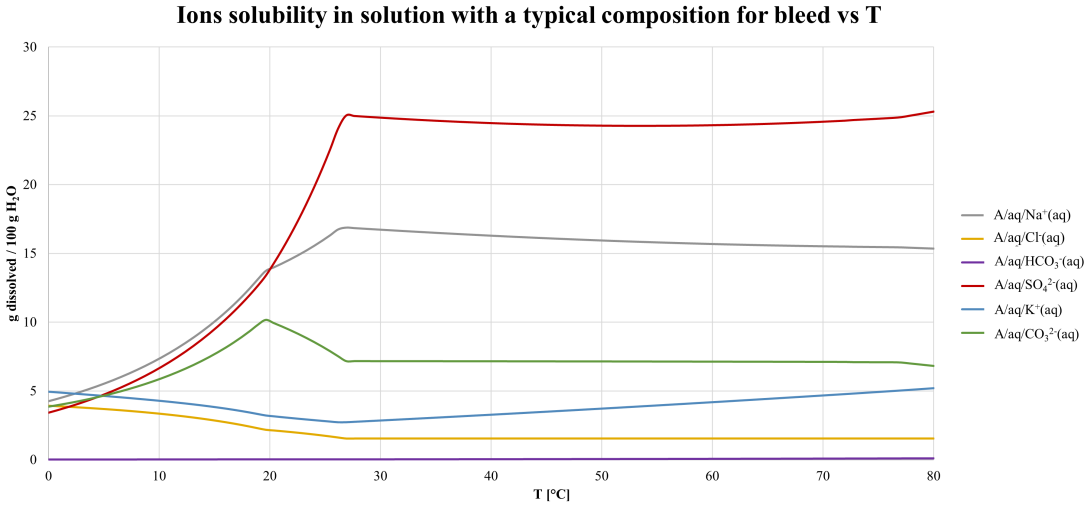

Figure 2.1: *Concentration of dissolved ions in Mill 1 bleed stream at different temperatures, indicating that solubility of potassium is at its lowest around 25 °C (adapted from Valmet, 2024, with permission).*

Furthermore, there are multiple proposals regarding the residence time as well. Since the bleed stream will be cooled, the residence time constitutes cooling time and reaction time. The residence time range is generally between 15-60 minutes [20]. In one example, it is mentioned that for a higher temperature, there should be a longer reaction time and vice versa [18]. In the same example, the recommended reaction times are at the shorter end of the mentioned interval. In another example, however, the suggested reaction time is at the longer end [17].

It is desired to obtain larger crystals rather than smaller [21]. Smaller particles are more difficult to separate, there is a larger risk of an increased amount of mother liquor adhering to the crystals. If too much mother liquor adheres to the crystals, more impurities remain. Hence, there would be an increased energy and equipment cost to manage the impurities. It is possible to control the size of the crystals during the process, through cooling rate. This is described in more detail in Section 2.1.1. It has been shown through previous research that a cooling rate of 0.2 °C/min is appropriate for the formation of Product A [22].

The mother liquor produced from the first step, ML1, can be recirculated in the same step to eventually increase the yield of Product B [15]. There are several suggestions on how the recirculation should be done. In one example, ML1 is subjected to evaporative crystallization to separate the sodium chloride [21]. The remaining mother liquor after evaporation is sent back to the first step. It is also suggested that the separated sodium chloride could be used in a membrane cell process in order to convert it into useful chemicals for the mill, sodium hydroxide, chloride, and hydrogen. Chloride and hydrogen could be utilized during the bleaching process or sold. Another example recommends directing ML1 to an anion segregation unit, such as nanofiltration, where a retentate, depleted in sulfate, and a permeate, rich in sulfate, is produced [19]. The retentate is recirculated back to the first step, while the permeate is directed to produce sodium chloride through crystallization.

The addition of sulfuric acid during the first step will reduce the amount of carbonates in Product A [16]. This is not necessary, but depends on the desired purity of the end product. If added to the aqueous mixture, the acid will react with the carbonates forming carbon dioxide, sulfates and water. The amount of added acid should be in an equivalent molar ratio to the amount of carbonates to be reduced. A subsequent step of pH modification, with potassium hydroxide or sodium hydroxide, may be used if the acid has been added to the process. This is to increase the pH and achieve a correct stoichiometric balance.

2.2.1.1 Competing Crystal Phases

Apart from the desired phase of Product A, it is possible that other phases may form during the cooling crystallization. This depends on temperature, solubility, pH, composition and water content [17]. One example of such a phase is hydrated sodium sulfate, also known as Glauber's salt. Usually, it is formed through a reaction between sodium chloride and sulfuric acid, but it can also crystallize at temperatures under 32 °C in an aqueous environment with the right circumstances [23]. Optimal conditions for this phase to form are in a rich sodium and sulfate solution, preferably with an excess of water. Because of the high water content in Glauber's salt, the crystals dissolve easily, and melt, at temperatures above 32 °C. Glauber's salt can also transform into sodium sulfate if water is evaporated.

Another potential competing phase is burkeite [24]. It is a double salt that can crystallize from an aqueous solution that contains sodium carbonate and sodium sulfate, and forms under non-optimal conditions for the formation of Product A. The temperature at which burkeite crystallizes is around 25 °C, however, the quality of the salt may differ depending on the composition of the solution. The elemental composition for Glauber's salt and burkeite is presented in Table 2.1.

Table 2.1: *Elemental composition of the two competing phases, in wt%. For Glauber's salt, the water is not included.*

Element [wt%]	Glauber's salt	Burkeite
Na	32.4	35.4
K	0	0
C	0	3.1
O	45.1	45.1
S	22.6	16.4
Cl	0	0

2.2.2 Step 2: Re-Crystallization of Intermediate Product A to Product B

The second part of the recovery is a re-crystallization step [15]. The unbalanced reaction is presented in equation (2.5).

$$\textit{Product A (s) + KCl (aq)} \rightarrow \textit{Product B (s) + NaCl (aq)} \tag{2.5}$$

Solid crystals of Product A and a saturated aqueous solution of potassium chloride are the starting materials of this reaction. There is no need for additional cooling, as the reaction mechanism occurs spontaneously when the starting materials are mixed. Crystals of Product A partly dissolves in aqueous potassium chloride. The sodium-rich salt dissolves while the potassium-rich salt remains in solid phase. As the solution is saturated, new crystals are formed through re-crystallization. These and the remaining crystals are Product B, and the byproduct is an aqueous sodium chloride solution. The saturated potassium chloride solution enhances the chances of obtaining purer crystals, as the potassium is in excess [15]. Therefore, it encourages the formation of Product B and drives the reaction towards the desired end product.

When using a bleed stream from a pulp mill, the reaction for Product B looks different in regards to components. The modified reaction is presented in equation (2.6).

$$\textit{Product A (s) + Salt solution (aq)} \rightarrow \textit{Product B (s) + Mother Liquor 2 (aq)} \tag{2.6}$$

As before, the reaction starts with solid crystals of Product A. However, they are partly dissolved in an aqueous salt solution. The end product is the desired Product B and the by-product is an aqueous salt solution, referred to as mother liquor 2, ML2. Multiple internal recirculation options of ML2 are possible. Recirculation in a process is preferred as it enhances resource efficiency and improves the yield [13]. ML2 can also be used to obtain further products, such as salts, as it contains several different ions, sodium and chloride among others [17]. After separation from Product B, it is possible to evaporate ML2 and attain these salts in solid form. The

salts can be utilized in various parts of the pulp mill or sold to other industries or companies.

Parameters that affect the reaction in the second step are temperature, residence time and concentration of solids [18]. The reaction is preferred to be performed when the saturated liquid is within the temperature range of 5-50 °C, it has been shown that higher temperatures negatively affect the yield of Product B [21][18]. The re-crystallization has been performed with residence times within the range of 15-60 minutes [20], but the formation rate of Product B generally decreases after 15 minutes, regardless of the temperature [18]. Thus, time is a factor that influences the process, but its importance is relatively minor, and the duration is generally shorter for the second step than for the first step. The concentration of solids is significant as it determines the efficiency of crystal formation [15]. However, if the solution is too concentrated, re-crystallization may occur too quickly, leading to crystals of poor quality.

2.2.3 Prior Experimental Results

In 2023 and 2022, experiments were performed on bleed streams from Mill 1 and Mill 2, respectively. The purpose of the experiments was to investigate the possibility to recover potassium from a bleed stream, which is relevant research for this project. This section will present results from the experiments and analyses made.

2.2.3.1 Crystallization of Product A with Bleed Stream from Mill 1 2023

Formation of Product A, through cooling crystallization, was successfully carried out once in 2023 with a bleed stream from Mill 1. Table 2.2 shows the composition of the bleed stream that was used, which had a DS of 37.1 %. The bleed stream was kept in a heating cabinet at 60-70 °C after collection.

Table 2.2: *Measured composition of the bleed stream from Mill 1 used for crystallization of Product A in 2023.*

Element	**Composition [wt%]**
K	3.82
Na	10.75
CO_3	4.04
SO_4	17.91
Cl	0.85
H_2O	62.6

Parameters from the experiment and the elemental composition of the obtained crystals are presented in Table 2.3 and Table 2.4, respectively. The DS of the crystals was 79.6 % and the final potassium recovery efficiency was 38.7 %.

Table 2.3: *Parameters used for crystallization of Product A in 2023 with bleed stream from Mill 1.*

Target Temperature [°C]	Average Cooling Rate [°C/min]	Reaction Time [min]
15	0.22	15

Table 2.4: *Measured composition of obtained crystals, Product A, in 2023. Obtained through analysis with ICP-OES.*

Element	Composition [wt% dry mass]
K	28.2
Na	13.5
CO_3	1.6
SO_4	56.9
Cl	0.4

2.2.3.2 Crystallization of Product A with Bleed Stream from Mill 2 2022

An attempt to crystallize Product A by using a bleed stream from Mill 2 was conducted in 2022. Table 2.5 presents the composition of the bleed stream, which had a DS of 30.0 %. The bleed stream was extracted from the mill and used in the experiment, without prior cooling. No solid phase could be observed at any stage during the experiment or filtration. Consequently, crystallization of Product A was not achieved.

Table 2.5: *Measured composition of the bleed stream from Mill 2 used for the attempt to crystallize Product A in 2022.*

Element	Composition [wt%]
K	3.3
Na	8.7
CO_3	5.9
SO_4	9.6
Cl	2.4
H_2O	70.1

2.2.4 Evaluation of Process Efficiency

When evaluating a process, it is important to investigate if it is an optimized, cost-effective and sustainable solution. This section will present and discuss factors involved in evaluating the process efficiency. One fundamental part is the crystallization efficiency, which indicates how effective the yield of crystals is [25]. For this

project, it will be based on how much of the bleed stream that is converted into dry crystals. The yield can be calculated according to equation (2.7)

$$\text{Yield} = \frac{\text{Crystals [g, dry]}}{\text{Bleed stream [g]}} \times 100\% \tag{2.7}$$

Additionally, the efficiency of the process can also be determined by evaluating the efficiency of potassium recovery in the crystals. This can be calculated according to equation (2.8).

$$\text{Potassium recovery efficiency [\%]} = \frac{\text{K in crystals [g, dry]}}{\text{K in bleed [g]}} \times 100\% \tag{2.8}$$

Another important aspect of the process efficiency is the particle size and purity of the crystal. As mentioned in Section 2.1.1, large and well-formed crystals are desired. Larger crystals indicate high purity and simplifies the solid/liquid separation. A well-controlled process, where factors such as temperature, supersaturation, and concentration are properly balanced is suggested. To achieve this, controlled cooling is necessary. There will be a balance of drawbacks and benefits, since slower cooling generates crystals with higher purity, however the process takes longer time. For a cost-effective process, it is desired to have a high output of product per time unit. Nevertheless, a process with slower cooling generally have a lower energy demand.

2.3 Evaluation of Energy Demand for Cooling Crystallization

As mentioned, the energy demand required for cooling during the crystallization in the first step will affect the overall process feasibility, as it is the major constituent of the total energy demand. Even though other processes would require energy, for example, solid/liquid separation, these are not accounted for in this project. The first step of the experimental phase is conducted in a jacketed batch reactor, a schematic drawing of this can be seen in Figure 2.2. A batch reactor operates as a non-continuous process, where the only independent variable is time. Other variables, such as temperature, are functions of time.

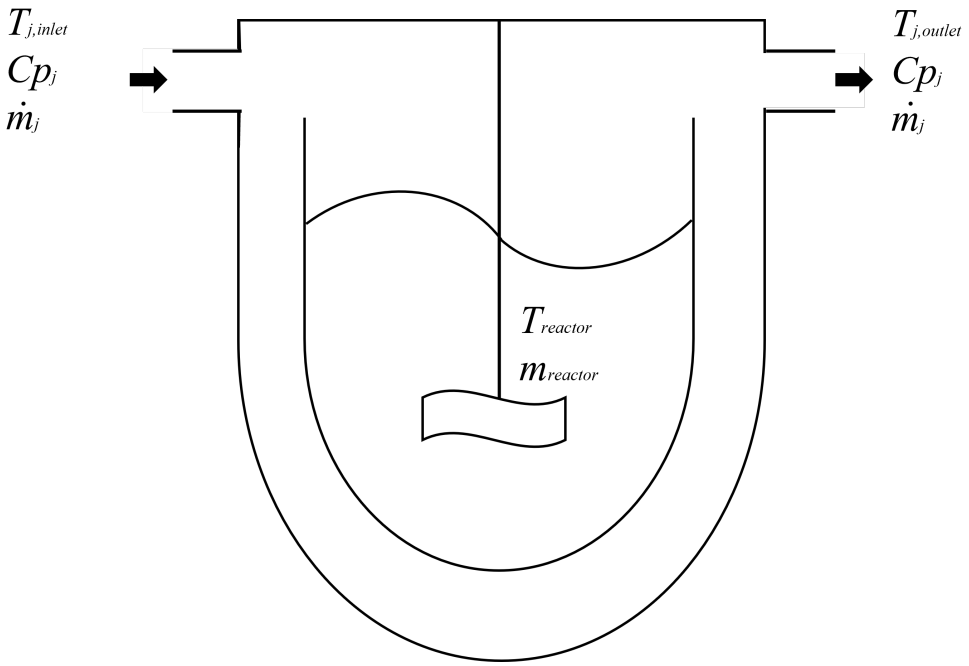

Figure 2.2: *A visualization of the jacketed batch reactor used during the first step of the experimental phase, known parameters are displayed.*

A cooling circuit is connected to the jacket of the reactor, a schematic drawing of the setup between the reactor and the cooling machine can be seen in Figure 2.3.

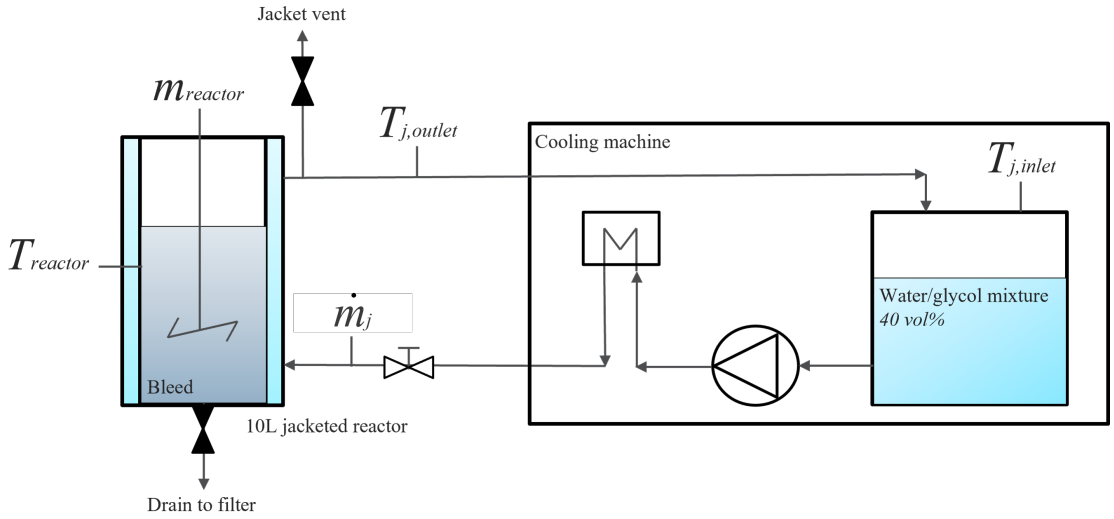

Figure 2.3: *The setup with the batch reactor and the cooling circuit.*

The inlet temperature of the cooling medium, $T_{j,inlet}$, is not fixed but decreases with time during the cooling process. This, since the cooling medium is at room temperature when the cooling machine starts. The bleed is gradually cooled, which indicates that the outlet temperature of the cooling medium, $T_{j,outlet}$, is also varying with time. The energy that is required for cooling the bleed stream can be integrated over time steps, to calculate the total energy demand for the whole process. Energy

required for cooling at a specific time step, t, is calculated according to equation (2.9) [26].

$$\dot{Q}_j(t) = (\dot{m}C_p)_j(T_{j,outlet}(t) - T_{j,inlet}(t)) \tag{2.9}$$

Where $\dot{Q}_j(t)$ is the heat transfer at that time step, in W, $(\dot{m}C_p)_j$ is the mass flow and specific heat capacity of the cooling medium in kg/s and J/(kg °C), respectively. Temperature is measured in °C, while time is expressed in s.

2.4 Conventional Production of Product B

Product B has conventionally been produced with potassium chloride and sulfuric acid [14]. The unbalanced reaction is shown in equation (2.10). The dominant by-product of that reaction is hydrochloric acid, which was formerly desired on the market. However, in recent years, the market for hydrochloric acid has diminished, and the production of Product B from natural salts has become more dominant.

$$KCl + H_2SO_4 \rightarrow Product\ B + HCl \tag{2.10}$$

Conventional production of Product B starts with adding the raw material into a furnace that is heated to 600 °C [14]. The raw materials react during slow mixing, where a plough is rotating to help with agitation. The resulting crystals and by-product are cooled, filtered, and then sold. Although the process is widely used for the production of Product B, it has many disadvantages. Firstly, it needs high temperatures for the reaction, which entails a high energy demand. This is both expensive for the company and unsustainable depending on the energy source. Secondly, there may also be some mechanical problems regarding corrosion on equipment from acids and chlorides. To prevent corrosion and frequent maintenance of the kiln, specialized equipment is required that can withstand direct flames, intense heat, and acid. As a result, the investment cost increases. Lastly, managing the gases from the by-product is also challenging due to the toxicity. Therefore, this process is not as preferred as it once was.

This project will evaluate a new process to produce Product B, specifically from a pulp mill. The two methods will be compared in regard to energy demand and process design. The energy demand of the conventional production of Product B was reported at 15.6 kJ/(g Product B) [27].

2.5 Analytical Methods

This section presents basic theory about the analysis methods which are going to be used during the experimental phase in this project.

2.5.1 XRD

X-ray diffraction, XRD, is a spectroscopic analysis method that can be used on solid samples. Diffraction is the physical phenomenon of interference produced through

the interaction of electromagnetic waves, for example, X-rays, and crystals [28]. When a beam of high-energy electrons is aimed at a metal target, X-rays will scatter [29]. These X-rays will obtain different wavelengths depending on the metal and are directed to the sample. The interference produced after this interaction is diffracted X-ray beams, which occur at specific angles [28]. Braggs's law describes the geometry of the diffraction, and can be seen in equation (2.11).

$$2d_{hkl} \sin\theta = n\lambda \tag{2.11}$$

The spacing between atomic planes in the crystals is expressed as d_{hkl}, λ is the wavelength of the incident X-rays and θ is half of the diffraction angle. At a given radiation wavelength of the X-rays, diffraction will only occur at angles where Bragg's law is satisfied. A diffractometer is used to measure the diffraction angle, 2θ, of the beams [29]. If the wavelength of the X-rays is known, the interplanar spacing can be determined. Subsequently, identification of the planes that caused the diffraction can be made. An XRD analysis identifies crystalline phases in a solid sample and quantifies them [28]. It also reveals information about the texture and orientation of these phases, how atoms and molecules are structured within a phase and the microstructure regarding crystallite size and strain.

D8 Discover Bruker XRD instrument was used in this project. Patterns are recorded with diffraction angle in the range of 2θ from 10° to 70°, with a scan step of 0.02°/s using the software DIFFRAC.EVA V5.2. The diffractograms were analyzed using the Crystallography Open Database.

2.5.2 SEM-EDX

Another analysis method that can be used on solid samples is scanning electron microscopy with energy-dispersive X-ray spectroscopy, SEM-EDX. SEM is an electron microscopy technique that can give information about surface topography, compositional distribution and qualitative versus quantitative information about chemical composition [30]. There is a high spatial resolution and a large depth focus which allows for three dimensional images with a lot of details about the topography. In the SEM there is an electron chamber and a sample chamber. In the electron chamber, primary electrons are generated by an electron gun. The electron beam is accelerated through electromagnetic lenses and apertures before reaching the sample. The sample chamber is equipped with a detector, for example an EDX.

SEM-EDX is generally used for determining chemical composition and the information is gained through characteristic X-ray energies. When a highly energetic electron ejects an electron in the inner shell of an atom, it will leave an empty space at a low energy level. An electron from a higher energy level, an outer shell, will relax and replace the ejected electron, the difference in energy between the levels will thus be released as an X-ray. The emitted X-ray is characteristic of the atom, from which the electron was ejected. The EDX detects the X-rays and creates a discrete spectrum. A FEI Quanta 200 FEG ESEM instrument was used in this project to

take SEM images. The images are recorded at 15 kV under vacuum. Some samples were dried before SEM-EDX analysis in a desiccator.

2.5.3 ICP-AES

Inductively coupled plasma atomic emission spectroscopy, ICP-AES, is used to determine the elemental composition in liquid samples [31]. The plasma is formed when a stream of argon gas is ionized, producing argon ions and electrons. As the electrons and argon ions move through the gas there will be some resistance, this is what causes the temperature to rise. Because of its high temperature, this method allows for a high atomization efficiency and population of excited states. All analytes in a sample are excited simultaneously, which makes ICP-AES a suitable method for multielemental analysis.

The sample, along with argon gas, is introduced to a nebulizer where a mist with µm-sized droplets are formed [32]. These droplets are carried by the argon gas, to the plasma induced torch. At the plasma, there is evaporation, atomization, excitation and ionization due to the considerable heat. While the excited atoms from the sample leave the high temperature zone in the torch, excited valence electrons relax and a photon is emitted. The emitted photon is specific to each element. The radiation emitted from the sample enters a monochromator, where characteristic wavelengths are separated and subsequently measured by a detector.

2.5.4 Dry solids analysis

The dry solids, DS, of a sample can be measured by measuring the mass difference of the sample after drying. When the sample is placed in the instrument it is weighed, this weight is considered as 100 %. As the temperature increases, the moisture in the sample will evaporate until the sample is dry. The sample will be considered dry when the mass no longer changes. The instrument calculates the DS, in %, of the original sample. This analysis can be executed on both solid and liquid samples. A LWP-MAA Moisture Balance was used for DS analysis. The drying temperature was set to 120 °C.

3
Methods

This chapter outlines the experimental and analytical methods employed in this project. It provides a description of the materials, procedures, and equipment used to investigate the feasibility to recover potassium. The methods that were used included a literature study, an experimental phase and an evaluation of the energy demand through MATLAB, as well as analytical methods. The experimental phase was performed at Valmet's laboratory in Torslanda, and the analyses of the solid samples were performed at Chalmers University of Technology in their Materials Analysis Laboratory. Liquid samples were sent to a commercial laboratory for analysis.

3.1 Literature Study on the Crystallization of Product A and Conversion to Product B

The project started with a comprehensive literature study to gain information, theories and data to base the experimental phase and evaluation on. The strategy for finding relevant sources was to search in databases, books, and patents on similar processes. A systematic search started with reports and technical articles that included the intermediate Product A, and the conversion to Product B. The literature study also included books and patents related to the recovery of potassium. They were used to understand the processes and theories behind the reactions. Although some sources were considered outdated and therefore less relevant, they still provided valuable insights. Patents were especially used to find relevant values for parameters, processes and data that had previously been effective to obtain the crystals in both experimental steps. Keywords used during search were for example the chemical names of both products, and cooling crystallization among others.

3.2 Experimental Plan

The experimental phase was divided into two different steps, with the goal of crystallizing Product A and Product B respectively. The first step of the experiment is described in Section 3.2.2, where the planned method for cooling crystallization of Product A is explained. After unexpected results, a modified method had to be constructed. This method is described in Section 3.2.4. The methods for the second step, re-crystallization of Product B, are described in Sections 3.2.6 and 3.2.7. Due to limited time and amount of Product A, there was a need for modifying this

method as well, as described in Section 3.2.8. The method for calculating the energy demand of cooling crystallization in MATLAB is described in Section 3.3.

3.2.1 Step 1: Materials

The materials for the first step were two bleed streams, 70 l was first collected from Mill 1 and 20 l was collected a month after from Mill 2, based on the results obtained for the bleed stream from Mill 1. The cans containing bleed stream from Mill 1 have a prefix of S, while the cans with bleed stream from Mill 2 have a prefix of F. The indexes for both mills are roman numbers. The bleed stream from Mill 2 had much more carry over from the recovery boiler than the one from Mill 1 and was therefore filtered before the start of the experiment, using vacuum filtration and double layered filter paper, with 40 µm particle retention. The DS of the bleed streams was analyzed with the TGA, and samples were prepared for elemental analysis. The containers with the bleed streams were stored at the laboratory in room temperature when not used. Prior to experiments, the bleed stream was heated in the heating cabinet set to 80 °C to increase its temperature and to try to dissolve any solids that have formed during storage. This was done to try to mimic the temperature and composition of the freshly collected bleed stream. Furthermore, a cooling medium was used with a mixture of 40 % glycol and 60 % water.

3.2.2 Step 1: Experimental Procedure

5 l of the bleed stream was weighed and poured into the reactor. The agitator was started and set to 200 rpm. Temperature logging was initiated using a Gemini Tinytag temperature probe. This probe was placed to monitor both the reactor temperature, $T_{reactor}$, and $T_{j,outlet}$. The data was recorded continuously at every minute throughout the experiment using the EasyView 12 software. $T_{j,inlet}$ was manually checked and noted every two minutes from the internal temperature indicator on the cooling machine. The cooling machine was turned on, the inlet temperature of the coolant to the jacket was set to a decided set point, depending on the desired cooling rate, and the cooling timer was started. To further regulate the cooling rate, the flow rate of the cooling medium was adjusted. When the target temperature was reached in the reactor, the cooling machine and cooling timer were turned off, and the reaction time started.

When the reaction time was reached, the filtration started. A Buchner set connected to a vacuum pump was placed under the reactor. A filter paper of size 20 cm and grade 4, with a particle retention of 25 µm was placed in the funnel. A porous stone with a glass sand core and 20-40 µm pore size was also added in the funnel to support the filtration process. The liquid in the reactor was drained from the reactor and filtered. The crystals ended up in the funnel and ML1 in the flask. The crystals and ML1 were collected in plastic containers and flasks with lids respectively. The masses were noted, and the DS was analyzed. Samples were prepared and liquids were sent to a commercial laboratory for elemental composition analysis with ICP-AES. The solid crystals were taken to Chalmers University of Technology to analyze

the elemental composition and take images, through SEM-EDX. To confirm phases, the crystals were also analyzed with XRD. All samples were stored in the laboratory at room temperature.

3.2.3 Step 1: Planned Experimental Matrix

The experiments were planned to be carried out with a full factorial design to investigate how parameters affected the yield of Product A. Depending on the run, the experiment had different values for the evaluation parameters, see Table 3.1. Using the results from the planned experiments, an optimization could have been performed where the conditions for maximized potassium recovery could have been determined. The parameters were chosen based on theory from Section 2.2.1. For both target temperature and reaction time, the intention was to evaluate how high and low values affect the potassium recovery efficiency. The size of the crystals depends substantially on the cooling rate, which is described in Section 2.1.1. It was therefore chosen to include a fast and slow cooling rate to investigate its impact on crystal formation in this experiment.

Table 3.1: *The planned experimental runs for the first step, with respective evaluation parameters for a full factorial design.*

Run	Target T [°C]	Reaction Time [min]	Cooling rate [°C/min]
1.a	25	60	fast*
1.b	25	60	slow*
1.c	40	60	fast*
1.d	40	60	slow*
1.e	5	60	fast*
1.f	5	60	slow*
1.g	25	15	fast*
1.h	25	15	slow*
1.i	40	15	fast*
1.j	40	15	slow*
1.k	5	15	fast*
1.l	5	15	slow*

*Specific cooling rates will be measured. Due to variations in other parameters, slow cooling rates may not be directly comparable with one another, nor fast cooling rates with other fast ones.

3.2.4 Step 1: Modifications to the Experimental Plan

During run 1.a, hereafter called 1.1, with the bleed stream from Mill 1, no crystal formation was observed in the reactor until at approximately 20 °C where Glauber's salt was formed instead of the expected Product A. Therefore, it was not feasible to

continue by following the planned full factorial experiment design for optimizing the recovery of Product A. Instead, the focus shifted to being able to find the conditions at which crystallization of Product A would be possible. The following modifications were implemented:

- During the experiment, the bleed stream was cooled to 15 °C and samples were taken out of the reactor at 32 °C and 25 °C. These temperatures were chosen since Glauber's salt precipitates at 32 °C, the solubility of potassium is lowest at 25 °C for the bleed stream from Mill 1 and the last successful experiment to crystallize Product A was done at 15 °C, see Section 2.2.1.1, 2.2.1 and 2.2.3.1 respectively.

- If there was a layer of crystals in the bottom of the sample, a fraction of the slurry from the reactor was filtered off. The mass of crystals and ML1 were noted, and samples were prepared for analysis. If no layer of crystals was observed, the sample was poured back into the reactor. Cooling of the remaining slurry in the reactor continued until 15 °C was reached, the slurry was then filtered as described in Section 3.2.2.

- When working with the bleed stream from Mill 2, the filter paper was changed to one with a particle retention of 40 µm, due to a high amount of carry over and poor filtration properties. Two filter papers were used, but the porous stone was not.

- From the results of run 1.7, 25 °C was defined as the optimal temperature for recovery of Product A, when using the bleed stream from Mill 2, see Appendix A.5 for calculations. The bleed stream was therefore cooled directly to 25 °C for the following experiments.

- XRD analysis was only conducted on two samples. Samples deemed sufficiently interesting based on SEM-EDX results were selected to confirm the crystalline phases.

Additionally, it was observed that a solid phase had precipitated in both bleed streams during storage at room temperature. These solids were difficult to re-dissolve, even after being heated in the heating cabinet at 80 °C for 12-48 hours. To promote dissolution, the solids were manually ground and mixed into smaller fractions of the bleed stream, then heated to higher temperatures on a heating plate. Nevertheless, it was not possible to completely dissolve the solids in the hot bleed stream. The liquid phase was decanted and used for further experiments while samples were collected. Solids that had formed during storage were collected and analyzed.

3.2.5 Step 2: Materials

The material for the second step was Product A from the two mills. Self-crystallized Product A formed in can SV during storage of the bleed stream from Mill 1 at room temperature was used, as there was no Product A recovered from this bleed stream

during cooling crystallization. For Mill 2, the crystals from run 1.7 at 15 °C were used. The crystals of Product A from the two mills differ a lot in structure and appearance since they have been crystallized under different circumstances.

To conduct a screening test for the second step, three saturated solutions were prepared. The solutions were a saturated solution of potassium chloride and a mimic of ML2 from both mills. To mimic ML2, water was saturated with Product A from the respective mill. For Mill 1, self-crystallized Product A from can SV was used. For Mill 2, crystals from run 1.9 were used. Saturated solution of potassium chloride was prepared from chemical grade solid potassium chloride. The solutions were created in big batches, and a few days before the experiments to ensure saturation. Since the solubility of the crystallized products is unknown, a test was performed to see how much of the respective product would be dissolved in water at room temperature. Based on this, the amount of Product A required to make a batch large enough to perform all experiments was calculated. Calculated values can be seen in Table 3.2. There were undissolved solids in all solutions after a few days, which were filtered off. The filtration set up was the same as the one used in the first step, see Section 3.2.2. For the measured values of the reactants and the DS of the final solutions, see the Appendix B.1 and Table B.2. The saturated solutions were used when preparing the leaching solutions.

Table 3.2: *Calculated amounts of water and added compound to produce the saturated solutions. The solutions containing Product A were prepared to mimic ML2.*

Solution	**Water [g]**	**Added compound [g]**
Sat. KCl	513.4	180.0
Sat. Product A Mill 1	708.3	151.6
Sat. Product A Mill 2	713.7	146.3

3.2.6 Step 2: Screening Test

Before conducting the full experiment, a screening test was planned in order to determine which leaching solution would be most suited to use for the re-crystallization. Six different leaching solutions were tested, these can be seen in the alphabetical list below. This method was applied to Product A from Mill 1 and Mill 2 to be able to make a comparison. The reason behind mimicking ML2 was to replicate a recirculation in the process, which is described in Section 2.2.2. It is also described that a higher potassium content will promote the formation of Product B, different mixtures of ML2, potassium chloride and water were therefore tested.

A: KCl saturated solution
B: 90/10 wt% mimic of ML2 & H_2O
C: 80/20 wt% mimic of ML2 & H_2O
D: 70/30 wt% mimic of ML2 & H_2O

E: 50/50 wt% mimic of ML2 & KCl saturated solution
F: 50/30/20 wt% mimic of ML2 & KCl saturated solution & H_2O

The screening test was conducted in a 250 ml plastic beaker, placed on a magnetic stirring plate. It was done with a 10 wt% dry solid content, for a 200 g solution. The amount of wet crystals needed for this concentration was calculated using the DS of the respective crystal, these were then placed in the beaker. Since there was some liquid trapped in the crystals, the required additional amount of respective solution was calculated. This was then added to the beaker as well, and the stirring started. The calculated quantities of each reactant to be added in respective experiments are shown in Table 3.3 and Table 3.4. All experiments were carried out for 30 minutes and the solution was subsequently filtered. The DS content was analyzed for the remaining crystals and corresponding ML2. Samples were prepared for further analysis of elemental composition.

Table 3.3: *Experimental details for the screening test using Product A from Mill 1. In these experiments, the ML2 mimic was prepared using the same Product A as that used in the experiments.*

Run	Leaching solution	Product A [g, dry]	Sat. KCl [g]	ML2 mimic [g]	H_2O [g]
2.2	A	21.7	178.3	—	—
2.3	C	21.7	—	142.6	35.6
2.4	E	21.7	89.2	89.2	—
2.5	F	21.7	53.5	89.2	35.7
2.6	B	21.7	—	160.5	17.8
2.7	D	21.7	—	124.8	53.5

Table 3.4: *Experimental details for the screening test using Product A from Mill 2. In these experiments, the ML2 mimic was prepared using Product A from the same mill as that used in the experiments.*

Run	Leaching solution	Product A [g, dry]	Sat. KCl [g]	ML2 mimic [g]	H_2O [g]
2.8	A	23.8	176.2	—	—
2.9	C	23.8	—	141.0	35.2
2.10	E	23.8	88.1	88.1	—
2.11	F	23.8	52.8	88.1	35.2
2.12	B	23.8	—	158.5	17.6
2.13	D	23.8	—	123.3	52.8

3.2.7 Step 2: Planned Experimental Matrix

This section describes how the method was originally planned to be executed for the second step of the experimental phase.

After the screening test, the two leaching solutions that performed best, i.e. the ones that resulted in most potassium recovery, were planned to be used for the full experiment. Other parameters for the second step were the temperature, concentration of solids in the solution and reaction time. Parameters that were planned to be tested for each run can be seen in Table 3.5 with a full factorial design. These were chosen based on theory from Section 2.2.2. The goal was to test the theory on how both high and low values of target temperature and reaction time affect the formation of Product B.

Table 3.5: *The experimental runs for the second step, with a full factorial design.*

Run	Leaching solution	Target T [°C]	Solid content [%]	Reaction Time [min]
2.a	1	20	10	15
2.b	2	20	10	15
2.c	1	40	10	15
2.d	2	40	10	15
2.e	1	20	30	15
2.f	2	20	30	15
2.g	1	40	30	15
2.h	2	40	30	15
2.i	1	20	10	45
2.j	2	20	10	45
2.k	1	40	10	45
2.l	2	40	10	45
2.m	1	20	30	45
2.n	2	20	30	45
2.o	1	40	30	45
2.p	2	40	30	45

200 g of the leaching solution was planned to be added to the 250 ml plastic beaker on a magnetic stirring plate. If the run was supposed to be conducted at 40 °C, the heating function on the stirring plate could be utilized. The temperature would have been measured with a temperature probe, connected to the Gemini Tinytag that automatically collects the temperature every minute. Required amount of wet crystals could be calculated with respective DS and added to the beaker. After adding the reactants to the beaker, the stirring as well as the reaction time would have started. The solution could then be filtered, and the DS content analyzed for both crystals and ML2. Samples would have been prepared for further analysis of elemental composition.

3.2.8 Step 2: Modifications to the Experimental Plan

Since there was an unexpectedly low amount of Product A and time for the second step of the experiment, the method for this had to be reconsidered as well, only the

screening test was performed.

3.3 Energy Demand Estimation for Cooling Crystallization in MATLAB

The energy demand for cooling crystallization was calculated and estimated using MATLAB. The code for the simulation is presented in Appendix C.1.

For the cooling medium, Cp_j was found to be 3.65 kJ/(kg °C), and the density was 1065.30 kg/m^3 at 20 °C and 1 bar [33]. They are assumed to be constant throughout the entire experiment, due to a relatively narrow temperature interval. It is further assumed that the reactor is adiabatic, since it is well insulated with the jacket and the experiment was conducted with a maximum duration of a few hours. The volumetric flow rate of the cooling medium has varied for the experiments. The flow rate has been set to either 11 or 2.5 l/min, for a fast and slow cooling rate respectively.

$T_{reactor}$ and $T_{j,outlet}$ were automatically logged with one-minute intervals. $T_{j,inlet}$ was manually logged at a two-minute interval, where an average increase was assumed to estimate the missing data point for the calculations. The time step for the calculations was set to 60 seconds, since it is the interval at which the temperatures were logged. The total time for cooling, where $T_{reactor}$ was cooled from the starting temperature to the target temperature, was recorded during the experiment. A time array was created with the total time divided into time steps. The logged temperatures were exported into Excel files, which were used to create temperature arrays.

At each time step, the cooling duty of the cooling medium, $\dot{Q}_j(t)$, was calculated according to equation (2.9). The total cooling duty, $\dot{Q}_j$, was then integrated with the built-in function *trapz*, over the total cooling time.

4
Results and Discussion

This chapter presents the results of the experimental phase and provides a discussion of their significance. It will give an understanding of the work process and why decisions were made depending on the results. The first section will look into the results and discussion for the first step, where the goal was to crystallize Product A. It will examine the process, present the analysis results and list the key findings. The second section presents the results from the second step of the experiment, where the goal was to re-crystallize Product B via intermediate Product A. It will discuss the screening test for six different leaching solutions and present analysis results. The estimation of the energy demand for the new process will be presented, and a comparison with the conventional process will be performed. Finally, an evaluation of the methods used will be made in the last section.

4.1 Results and Discussion: Step 1

This section presents the results and discussion regarding the first step of the experiment. It will go through the results of crystallization with the bleed stream from Mill 1 and Mill 2. After every experiment, solid and liquid samples were taken. Since the results for these were delayed a few weeks, theories and hypotheses were confirmed or refuted in retrospect.

To see exact experimental measurements regarding for example specific weights and DS for all experimental runs, see Appendix A.1.

4.1.1 Cooling Crystallization of Bleed Stream from Mill 1

The experiment started with performing run 1.1, according to the method in Section 3.2.2. During filtration, there was formation of a thick slurry with a lot of crystals. This made filtration difficult and the whole funnel was filled with crystals to the brim, see Figure A.1 in Appendix A.2. The results of run 1.1, and following runs executed with the bleed stream from Mill 1, can be seen in Table 4.1. The crystals from run 1.1 showed an average DS of 42.2 % which indicated that there had not been formation of pure Product A. The crystals were instead believed to be Glauber's salt, since they had a high liquid content, which was indicated by the DS, and melted easily. This was also confirmed by the solid analysis, see Table 4.2. Furthermore, the last successful experiment using the bleed stream from Mill 1, conducted in 2023, produced crystals with a much higher DS, see Section 2.2.3.1.

Table 4.1: *Summary of experimental settings and results for executed runs on the bleed stream from Mill 1.*

Run	**1.1**	**1.2**	**1.3**	**1.4**	**1.5**
Cooling rate$_{avg}$ [°C/min]	0.88	—	0.26	0.34	0.28
Coolant flow rate [l/min]	11	11	2.5	2.5	2.5
T$_{j,inlet}$ set point [°C]	0	0	0/5*	5/10*	10/5*
Final temperature [°C]	25	15	15	15	15
Crystals present at 32 °C	No	No	No	No	No
Crystals present at 25 °C	Yes	Yes	No	No	No
Crystals present at 15 °C	—	Yes	Yes	Yes	Yes
DS$_{avg}$ crystals [%]	42.2	40.9	44.0	42.4	44.8
DS of bleed [%]	31.2	31.2	33.5	32.2	31.5
Can of bleed	SI	SI/SII	SII	SII**	SIII
Solids formed in bleed during storage	No	No	Yes	Yes	Yes

*The set point for T$_{j,inlet}$ was changed during the experiment, to adjust the cooling rate. **This bleed stream was spiked with KCl before the experiment was conducted.

Run 1.2 to 1.5 were carried out according to the modified method in Section 3.2.4, in order to investigate if crystallization of Product A with the bleed stream from Mill 1 was possible under any circumstances. The goal of run 1.2 was to see when the eventual crystals of Product A would form. At 32 °C, no crystals could be seen and at 25 °C the slurry in the reactor was thin and the crystals were very small. At 15 °C the slurry was thick, and the walls of the reactor were covered in crystals. When the slurry was filtered, the funnel was filled with crystals as in run 1.1. This occurred for all following experiments with the bleed stream from Mill 1. Some of the crystals from run 1.2 melted easily and some were stable, leading to the belief that it could be a mixture of Product A and a competing phase. The DS also indicated that it was not pure Product A, see Table 4.1. This led to a hypothesis that there was not enough time for the crystals of Product A to be formed, i.e. that the cooling rate was too fast. Based on the fact that the experiment performed in 2023 had a cooling rate of 0.24 °C/min, see Section 2.2.3.1. It has also been shown in literature that this is suitable for the first step, which can be seen in Section 2.2.1. The average cooling rate was significantly higher than this in run 1.1, where it was approximately 0.88 °C/min, see Table 4.1. For run 1.2, no average cooling rate could be calculated, since the experiment was done in multiple steps of cooling and filtration, and the cooling machine was repeatedly turned on and off. However, the same settings were used for the cooling circuit as in run 1.1.

Before conducting run 1.3, approximately 180 g solids were found in can SII, these can be seen in Figure 4.1. It was later found in all cans. There were no solids in the bleed stream when it was collected from the mill, so it had been precipitated during storage at room temperature over a long time. The can of bleed stream that was used for the first experiments, SI, had no precipitated solids in it after storage. It

had been stored at room temperature for 5 days, while can SII had been stored at room temperature for 14 days, before being used. This implies that the solids that precipitated in room temperature did so with slow cooling, within a time period of 5 to 14 days. These solids were confirmed to be Product A, see Table 4.3. There were no signs of Glauber's salt in the cans, which indicates that the formation of Product A is favored over the formation of Glauber's salt when very slow cooling is applied. Attempts were made to dissolve the solids by increasing the temperature, but it was not possible to dissolve all of it and the bleed stream was therefore believed to be saturated. The solids that did not dissolve were separated from the liquid before the experiment started. For run 1.3, the cooling rate was decreased by first decreasing the volumetric flow rate of the cooling medium, while the set point of $T_{j,inlet}$ remained at 0 °C. In an attempt for a further decreased cooling rate, the set point was increased to 5 °C during the experiment. Again, the DS of the crystals indicated that it was not purely Product A, see Table 4.1. This led to the belief that there might not be enough potassium in the bleed stream to crystallize Product A.

Figure 4.1: *Solids found in can SII before run 1.3.*

Before run 1.4, 80 g of potassium chloride was added into the bleed stream in an attempt to increase the potassium content. The mixture was left overnight in the heating cabinet at 80 °C, however, most of the potassium chloride was left undissolved at the bottom of the can. Solids were decanted and the spiked bleed stream was used for run 1.4. The crystals obtained were soapy and small and had a DS similar to the previous experiments, see Table 4.1.

It was noted that the heat transfer from the heating cabinet to the bleed stream was not very effective, the temperature of the bleed stream was significantly lower than what the cabinet was set to. It was therefore believed that this might have been the reason why the solids did not dissolve in previous attempts. Before run 1.5, attempts were made to dissolve the precipitated solids from can SIII according

to the method in Section 3.2.4, but they were unsuccessful, and the experiment was started anyway. The obtained crystals had a DS of 44.8 %, see Table 4.1. After these last experiments, it was understood that neither potassium chloride nor the solids would dissolve in the bleed stream, presumably because it was already saturated with other salts. Since the solids did not even dissolve at the temperature the bleed stream had in the mill, it was believed that the bleed stream was supersaturated when collected. Therefore, it was assumed that further dissolution of potassium into this bleed stream would not be possible.

Crystals from run 1.1 to 1.5 and can SII and SV were analyzed with SEM-EDX. The results from these analyses can be seen in Table 4.2 and Table 4.3, respectively. These tables only contain a selection of spectra from the analyses. For all analysis data, see Tables A.2 and A.3 in Appendix A.3.

Table 4.2: *Selection of spectra with the elemental composition of crystals from the experimental runs with bleed stream from Mill 1.*

Element [wt% dry mass]	**1.1***	**1.2***	**1.3**	**1.4**	**1.5***
Spectrum					
K	1.9	0	1.1	2.1	0
Na	31.2	18.1	31.2	33.9	33.4
C	4.5	20.5	4.3	0	0
O	43.3	34.0	42.6	44.2	44.6
S	16.9	27.3	19.4	18.6	21.9
Cl	2.2	0	1.3	1.1	0
Spectrum					
K	1.2	1.1	31.6	25.4	0
Na	33.5	28.5	8.4	12.7	31.8
C	4.7	10.2	4.1	2.9	3.6
O	41.3	43.6	37.4	41.9	44.2
S	15.8	15.9	18.6	16.0	20.4
Cl	3.5	0.7	0	1.1	0
Spectrum					
K	1.2	0	28.3	—	24.8
Na	30.5	31.2	10.2	—	15.3
C	5.5	3.5	5.8	—	0
O	41.9	42.7	37.6	—	42.7
S	20.0	22.6	18.1	—	26.8
Cl	0.9	0	0	—	0

*The samples were dried before being analyzed with the SEM-EDX.

It can be seen from Table 4.2 that the crystals from run 1.1 and 1.2 had no spectra with a high potassium content. When compared to the concentration of potassium in the crystals from the experiment conducted in 2023, it was concluded that crys-

tals from run 1.1 and 1.2 could not be Product A. For the crystals from 1.3, two different phases could be observed, see Figure 4.2. There is a distinct difference in the appearance of the crystals that have a high potassium content compared to the ones with a low potassium content. The crystals with a high potassium content seem to be Product A, based on the chemical composition. It can be concluded that more potassium has been crystallized in run 1.3, compared to 1.1 and 1.2. Run 1.3 was the first experiment where the cooling rate was decreased, which indicates that it can be an important factor for the formation of Product A. Two different phases could also be observed in the crystals from run 1.4, similar to the ones in run 1.3. In the crystals from run 1.5, multiple phases were present as well, where one could be Product A. For samples that were dried before being analyzed, all water would have been evaporated, therefore, Glauber's salt will present as sodium sulfate in the analysis. There are spectra that clearly show as sodium sulfate, especially in the crystals from run 1.5. It is clear that competing phases and trapped ML1 were present in several samples, with potential contamination by potassium, carbon, and chloride likely originating from ML1. Trapped elements will affect the concentration of other elements to appear lower than they actually are. Burkeite might have been crystallized as well, however, it is less likely since Glauber's salt crystallizes at higher temperatures. The assumption is made based on the comparison with the chemical compositions for the respective compound, and theory in Section 2.2.1.1.

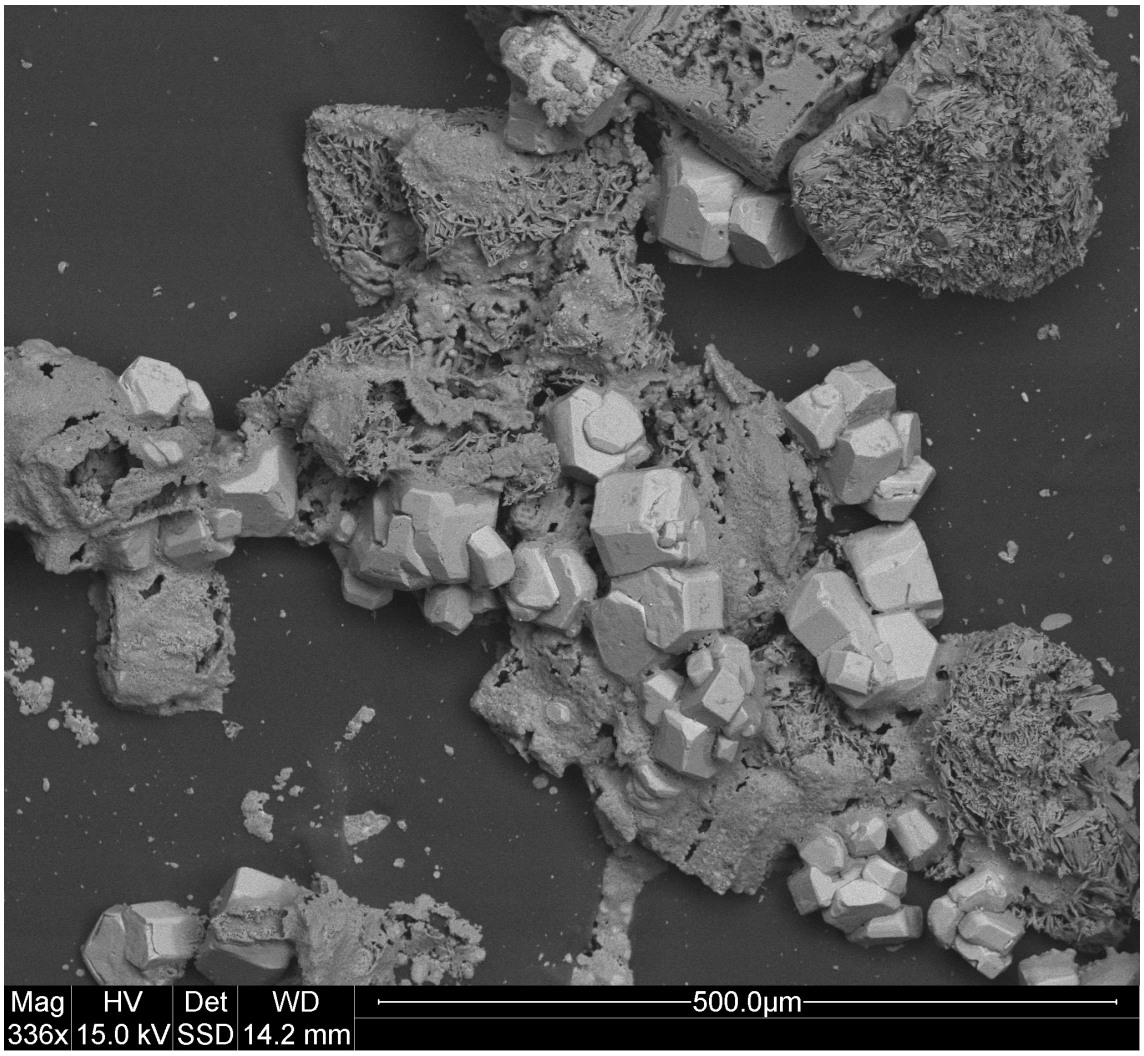

Figure 4.2: *Image of crystals obtained in run 1.3, taken with SEM-EDX. The smaller and lighter crystals are higher in potassium content, while the darker ones are low in potassium.*

It was found that a significant amount of potassium had precipitated during storage in room temperature, see Table 4.3. Since it was unsuccessful to re-dissolve the solids into the bleed stream, it could explain why an unexpectedly low amount of potassium crystallized during the experiments. Based on the elemental composition and that the DS of the solids was 94.6 %, it can be concluded that it is Product A.

Table 4.3: *Selection of spectra from SEM-EDX analysis of the self-crystallized solids from cans containing bleed stream of Mill 1.*

Element [wt% dry mass]	**SII**	**SV**
Spectrum		
K	11.4	30.0
Na	19.2	9.4
C	11.5	2.7
O	37.3	40
S	20.0	17.6
Cl	0.6	0.3
Spectrum		
K	23.3	28.8
Na	14.4	11.1
C	3.7	3.3
O	42.1	38.4
S	16.1	17.9
Cl	0.4	0.4
Spectrum		
K	30.5	20.8
Na	9.0	17.2
C	9.2	3.7
O	32.3	40.4
S	18.6	16.8
Cl	0.4	1.2

Table 4.4 shows the results from the liquid analysis, with ICP-AES, of the bleed stream from Mill 1. Compared to the composition from the experiment in 2023, see Table 2.2, it is observed that the concentration of potassium, sodium and sulfate is overall lower in the bleed stream used during these experiments. Furthermore, there is a considerable difference in IAP between the bleed streams, see Table 4.9. This confirms that the bleed stream used for run 1.1 to 1.5 was not nearly as saturated with Product A. The crystallization of Product A was therefore not likely with this composition and the experimental conditions. No solids had self-crystallized from can SI, nevertheless, Product A was not formed during run 1.1 or 1.2. This implies that it would not have been possible to further crystallize Product A with this bleed stream and conditions, even if the dissolution of the solids would have been successful. It can be seen in Table 4.4 that there has been a small increase of potassium in the can which was spiked with potassium chloride, it was however concluded that not much was dissolved. This is also supported by the analysis of the crystals from

run 1.4, which did not contain more potassium than the crystals from run 1.3.

Table 4.4: *Elemental composition and DS of the bleed stream from Mill 1.*

Element [wt%]	**SI**	**SII**	**SII (spiked with KCl)**
K	2.49	2.61	2.85
Na	8.65	10.112	9.51
SO_4	15.89	17.77	16.37
DS [%]	31.2	33.5	32.2

A mass balance over potassium for all experiments performed with the bleed stream from Mill 1 can be seen in Table 4.5. The mass balance was created with the results from the liquid analysis, these can be seen in Table A.5 in Appendix A.4. It is observed that a lot of the potassium remained in ML1, but some potassium ended up in the crystals as well. However, it is difficult to know if this potassium has been crystallized or trapped as ML1 in the crystals. The efficiency of potassium recovery in the crystals from run 1.1 and 1.2 is low, which aligns with the results from the analysis with SEM-EDX. It can be seen in Table 4.5 that the potassium recovery efficiency is higher for the crystals obtained in run 1.3 and 1.4. Since these crystals seem to be a mixture of Product A and another phase, some potassium has been crystallized during the experiment. However, a part of it results from trapped ML1. Run 1.5 is not included in the table as the bleed stream used during that experiment was not analyzed.

Table 4.5: *Mass balance over potassium for experiments conducted with the bleed stream from Mill 1.*

Run	**K in bleed [g]**	**K in ML1 [g]**	**K recovery efficiency in crystals [%]**
1.1	169.99	153.31	9.8
1.2	116.28	105.32	9.4
1.3	178.39	120.85	32.3
1.4	132.90	99.06	25.5

4.1.1.1 Key Findings: Cooling Crystallization - Mill 1

Findings from the experiments and analyses of run 1.1 to 1.5 will be presented in this section. They are based on the results that were disclosed during the first step of the recovery, where the bleed stream from Mill 1 was used to crystallize Product A. The most important findings are listed below.

- Slow cooling is an important factor. It is seen that the crystals with lowest concentration of potassium are those cooled with the fastest cooling rate.

Highest potassium concentration is found in the crystals cooled with the slowest cooling rate. Furthermore, the potassium recovery efficiency was improved by slower cooling.

- Bleed stream composition is an important factor. It is not possible to crystallize Product A with all compositions. The composition of the bleed stream can highly depend on the plant's operational conditions.
- Product A crystallizes by itself from this bleed stream when being cooled in room temperature over a time period of 5 to 14 days.
- Slow cooling presumably favors the formation of Product A before competing phases.

4.1.2 Cooling Crystallization of Bleed Stream from Mill 2

The bleed stream from Mill 2 was used in five different experiments. The experimental results for these can be seen in Table 4.6.

Table 4.6: *Summary of experimental settings and results for executed runs on the bleed stream from Mill 2.*

Run	**1.6**	**1.7**	**1.8**	**1.9**	**1.10**
Cooling rate$_{avg}$ [°C/min]	0.39	0.34	0.72	0.84	1.03
Coolant flow rate [l/min]	2.5	2.5	2.5	2.5	11
T$_{j,inlet}$ set point [°C]	10	10	10	10	10
Final temperature [°C]	15	15	25	25	25
Crystals present at 32 °C	No	Yes	No	Yes	Yes
Crystals present at 25 °C	No	Yes	No	Yes	Yes
Crystals present at 15 °C	No	Yes	No	—	—
DS$_{avg}$ crystals [%]	—	92.5	—	83.9	90.9
DS of bleed [%]	28.7	31.0	29.1	33.3	32.2
Can of bleed	FI	FI*	FII	FII*	FII*
Solids formed in bleed during storage	Yes	Yes	Yes	Yes	Yes

*After dissolution of precipitated solids.

Before run 1.6, 590 g of solids were found in can FI, similar to the ones found in the bleed stream from Mill 1. This can had been stored in the heating cabinet overnight, after being kept at room temperature for 12 days. Attempts of dissolution were made, but they were unsuccessful. The experiment was conducted after removing the solids. When the target temperature was reached, no crystals had been observed in the reactor. The filtration was very time-consuming, due to carry over from the recovery boiler blocking the filter paper. After the filtration, it was concluded that

there had been no crystallization. This could be a result from the fact that the DS of the bleed stream was 28.7 %, which is quite low, suggesting that the bleed stream was undersaturated. A new attempt was made to dissolve the removed solids in can FI, according to the method in Section 3.2.4. This time, the temperature increased more than in previous attempts, and the solids seemed to be dissolving slowly. The can of bleed stream was then stored together with the remaining solids in the heating cabinet at 80 °C for approximately 40 hours. When run 1.7 was to be executed, solids had been dissolved, and the DS had increased to 31 %. The sample taken at 32 °C during the experiment revealed a layer of crystals, see Figure 4.3a, and a fraction of the slurry was therefore filtered.

(a) *A layer of crystals seen at the bottom of the sample taken at 32 °C, in run 1.7.*

(b) *Crystals obtained from run 1.3 with bleed stream from Mill 1 at 15 °C, believed to be a mixture of Glauber's salt and Product A.*

(c) *Crystals obtained from run 1.7 with bleed stream from Mill 2 at 32 °C, believed to be Product A.*

Figure 4.3: *Top image shows the layer of crystals in the sample of 1.7 at 32 °C. The bottom two images are of crystals from different runs and mills.*

The crystals obtained at 32 °C had a DS of 85.6 %, which indicated that it was Product A. A layer of crystals was also present in the sample taken at 25 °C, and a fraction of the slurry was filtered. These crystals had a DS of 85.9 %. The remaining slurry was filtered at 15 °C, the obtained crystals had a DS of 95.7 %. The average DS of the crystals from run 1.7 was calculated to 92.5 %, see Table 4.6. For a comparison of the appearance between the crystals obtained in run 1.3 and 1.7, see Figures 4.3b and 4.3c.

Now that crystallization of what is believed to be Product A was possible, the temperature for maximum yield could be determined. These calculations were made according to equation (2.7) and can be seen in Appendix A.5. The maximum yield was decided to be at 25 °C, although it was very similar at 32 °C. For 15 °C it was significantly lower. However, these calculations might be deceptive. There is a possibility that crystals had sedimented before filtration, despite the agitation, which could be a reason for the yield being very low at 15 °C compared to the other temperatures.

When can FII had been stored in room temperature for 15 days, 806 g of solids was found inside it. To dissolve them, the method described in Section 3.2.4 was applied. The DS of the bleed stream was measured to 29.1 % before run 1.8 was started. Since a significant amount of the solids had been dissolved, the experiment was proceeded, even though the DS was lower than desired. Similar to run 1.6, no crystals formed, which is believed to be a result of an insufficient amount of undissolved solids. Seen in Table 4.6, the DS of the bleed stream for run 1.6 and 1.8 were similar. Since the DS was below 30 % both times, and solids were found in the bleed stream before each experiment, it implies the bleed stream once again is undersaturated. Considering that nothing had been crystallized, the bleed stream was poured back into can FII and kept in the heating cabinet overnight. Since the DS was still below 30 % the next day, the method for dissolution, described in Section 3.2.4, was applied again. Thereafter, the DS had increased to 33.3 % and run 1.9 was started.

Run 1.9 and 1.10 were both conducted to the same target temperature, however, they were intended to follow slow and fast cooling rates, respectively. Seen in Table 4.6, the cooling rate for run 1.9 was increased, compared to 1.6 and 1.7, even though the same settings were used for the cooling machine. This is mostly due to the fact that the target temperature was 25 °C, instead of 15 °C. A larger temperature difference increases the driving force for cooling, resulting in a higher cooling rate. To achieve a fast cooling rate for run 1.10, the flow rate of the cooling medium was increased to 11 l/min. However, the cooling rate did not differ as much as expected between run 1.9 and 1.10. Nevertheless, there was a big difference in the mass of the crystals obtained. Run 1.9 obtained 451 g of wet crystals, while run 1.10 obtained 261 g of wet crystals. A calculation of the yield was performed using the same procedure as in Appendix A.5, according to equation (2.7). This resulted in a yield of 5.55 % and 3.58 %, for run 1.9 and 1.10, respectively. To compare the amount of crystals obtained after filtration from experiments using bleed stream from Mill 1 and Mill 2, see Appendix A.2 and Figures A.1 and A.2.

Crystals obtained in run 1.7, run 1.9 and run 1.10 were analyzed with SEM-EDX. Table 4.7 presents a selection of the spectra from the analysis. For all analysis data, see Table A.4 in Appendix A.3. The spectra shown in Table A.4 are consciously chosen to show that there were different types of crystals in the sample. They do not show a fair representation of the quantity of these types of crystals. In Appendix A and Table A.3, analyses for the solids found in can FI are also presented. The

compositions from those spectra resemble the other solids found in cans from Mill 1, and are in all probability also self-crystallized Product A.

Table 4.7: *Selection of spectra with the elemental composition of crystals from experimental runs with bleed stream from Mill 2.*

Element [wt% dry mass]	**1.7** 15°C	**1.7** 25°C	**1.7** 32°C	**1.9**	**1.10**
Spectrum					
K	35.3	33.5	39.6	32.8	35.9
Na	7.9	10.8	6.6	9.7	9.1
C	0	0	0	0	0
O	36.4	38.1	31.5	36.3	33.1
S	20.4	15.9	22.2	19.8	21.9
Cl	0	1.7	0	1.4	0
Spectrum					
K	32.4	30.7	33.8	26.3	32
Na	8.9	10	10.5	10.9	9.9
C	0	0	0	0	0
O	39.1	40.3	34.8	46	38.2
S	19.1	19	15.8	16.8	19.9
Cl	0.5	0	5	0	0
Spectrum					
K	2.4	3.3	13.5	15.1	3.3
Na	29.5	29.6	13.5	22.5	29.3
C	7.5	6.8	0	4.9	6.3
O	39.6	42.3	40.5	37.3	40.2
S	16.8	14.3	32.5	14	18.3
Cl	4.2	2	0	6.1	2.7

As can be seen in the Table 4.7, there is generally a higher concentration of potassium in crystals that were obtained from the bleed stream from Mill 2 compared to Mill 1, see Table 4.2. However, there are still some locations within these samples where crystals with low potassium concentration can be found. The numbers of spectra showing a high potassium content exceed the number of spectra showing a low content, which can be seen in Table A.4 in Appendix A.3. Most of the spectra display a chemical composition that corresponds to the molecular compound of Product A. Furthermore, the composition is quite similar to the one of the crystals obtained in the experiment from 2023, see Table 2.4. The crystals obtained using bleed stream from Mill 2 are therefore in all probability Product A. Figure 4.4 shows images of crystals from run 1.7 at three different temperatures.

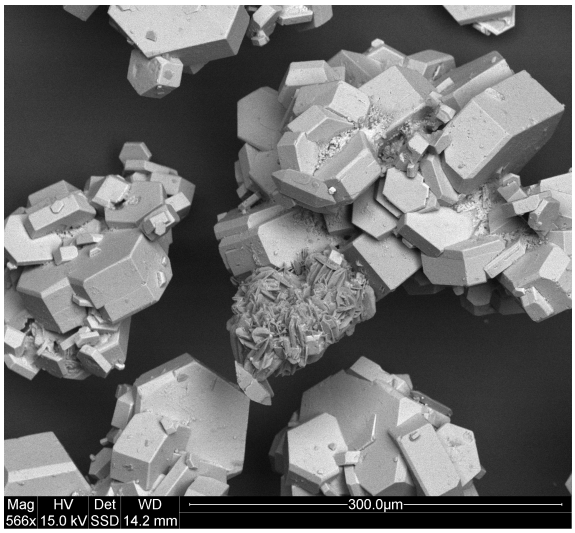

(a) *Image of crystals from run 1.7 at 15 °C.*

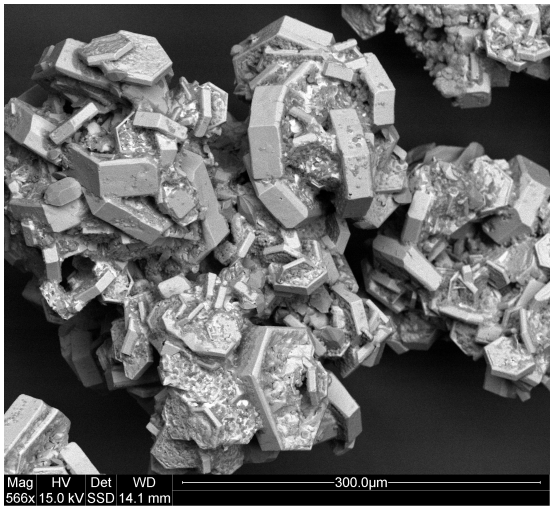

(b) *Image of crystals from run 1.7 at 25 °C.*

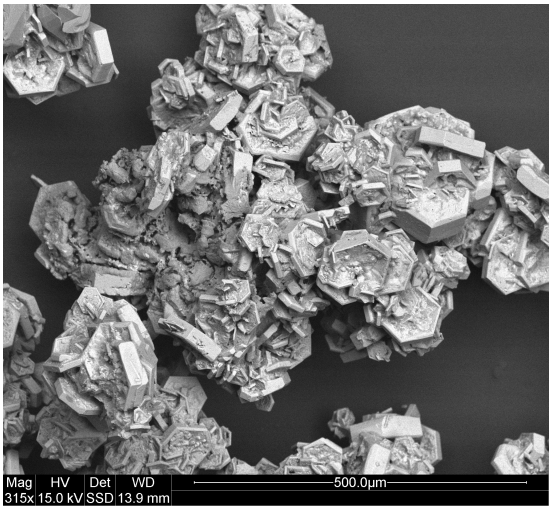

(c) *Image of crystals from run 1.7 at 32 °C.*

Figure 4.4: *Images of obtained crystals from run 1.7 at three different temperatures, taken during SEM-EDX analysis.*

Figure 4.4a highlights that the crystals are more developed at 15 °C, compared to the other temperatures in Figures 4.4b and 4.4c. The development of the crystals appears to be connected to a decreased temperature, a longer residence time, or a combination of both. In Figure 4.4a two phases are present, where the majority are crystals with a high potassium content, Product A. For a comparison, see Figure 4.2 which shows an image of the crystals obtained in run 1.3. In that figure, some Product A is visible, but there are also many crystals with a low potassium concentration.

Table 4.8 presents the results from the ICP-AES analysis of the bleed stream from Mill 2. A sample from can FI, which was used for run 1.7, was taken and sent to

analysis. However, due to an issue that occurred during the analysis, the results are considered unreliable and not applicable. There is a higher concentration of potassium, sodium and sulfates in can FII, after dissolution, compared to the other cans in the table. Furthermore, there is generally a higher concentration of potassium, and a lower concentration of sulfates, in the bleed stream from Mill 2 compared to the bleed stream from Mill 1. These conditions may have contributed to the crystallization of Glauber's salt during the experiments with bleed stream from Mill 1. The IAP, with regards to Product A, has been estimated with molar concentrations, according to equation (2.2), this can be seen in Table 4.9. The calculations will not be disclosed, as they contain confidential information. It can be observed that when Product A was crystallized during run 1.9, 1.10 and the experiment in 2023, the bleed stream had a high IAP with regards to Product A. During run 1.6, 1.8 and the experiment in 2022, where nothing was crystallized, the bleed stream had a low IAP with regards to Product A.

Table 4.8: *Elemental composition and DS of the bleed stream from Mill 2.*

Element [wt%]	**FI**	**FI***	**FII**	**FII***
K	3.29	—	3.35	4.34
Na	8.87	—	8.79	9.13
SO_4	8.63	—	8.80	10.45
DS [%]	28.7	31.0	29.1	32.2-33.3

*After dissolution of precipitated solids.

Table 4.9: *Estimated IAP for different samples of bleed stream from Mill 1 and Mill 2.*

Bleed stream	**IAP**	**Run**
SI	310.6	1.1, 1.2
SII	872.1	1.2, 1.3
SII (spiked with KCl)	941.3	1.4
Old, 2023 Mill 1	10049.0	—
FI	97.0	1.6
FII	113.2	1.8
FII*	1162.0	1.9, 1.10
Old, 2022 Mill 2	142.7	—

*After dissolution of precipitated solids.

A mass balance over potassium for all experiments performed with the bleed stream from Mill 2 can be seen in Table 4.10. This was created with the results from the liquid analysis, which can be seen in Table A.6 in Appendix A.4. For run 1.9 and

1.10 it is concluded that the recovered potassium in the crystals has been crystallized during the experiment. This is based on the results from the SEM-EDX analysis, where most locations within the sample showed crystals with a high potassium concentration. The potassium recovery efficiency, see Table 4.10, is similar to the one obtained during the experiment in 2023. Once again, the run with slow cooling, 1.9, is preferable as it achieved higher efficiency than the run with fast cooling, 1.10. The potassium recovery efficiency for run 1.9 and 1.10 is also resembling the efficiency for run 1.3. This is probably due to a significantly larger amount of crystals being obtained in run 1.3 compared to run 1.9 and 1.10. It is therefore a higher possibility for ML1 to be trapped in crystals from run 1.3, the potassium recovery efficiency should be lower for that experiment. Due to the error in the analysis of the bleed stream used in run 1.7, a potassium recovery efficiency could not be calculated for this run.

Table 4.10: *Mass balance over potassium for experiments conducted with the bleed stream from Mill 2.*

Run	**K in bleed [g]**	**K in ML1 [g]**	**K recovery efficiency in crystals [%]**
1.9	295.9	198.1	33.0
1.10	287.6	199.4	30.7

The crystals from run 1.7 at 15 °C were also analyzed using XRD, where the results confirm that the sample almost completely consists of Product A. The diffractogram from the analysis can be seen in Figure 4.5. The red peaks indicate the presence of the intermediate Product A, and evidently red is visible in all peaks of the diffractogram. It was not possible to analyze more samples with XRD, although, it would have been interesting to analyze crystals from 1.7 at 25 and 32 °C as well to see if those solely would have consisted of Product A as well. However, Figures 4.4b and 4.4c indicate that those crystals might not be as pure as those obtained at 15 °C. Based on the similarities between the crystals, and SEM-EDX results, it is assumed that crystals from run 1.9 and 1.10 also consists almost entirely of Product A.

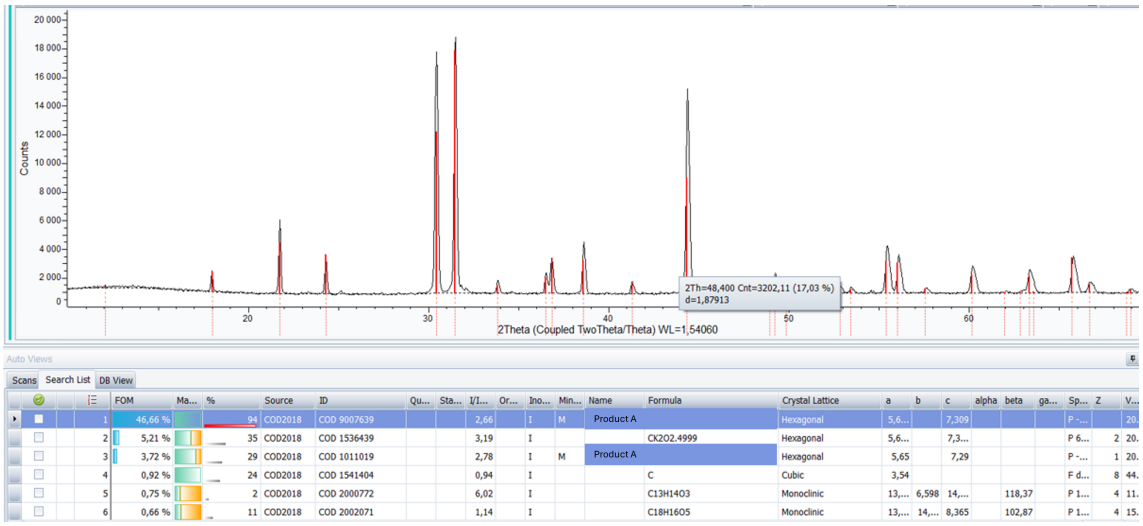

Figure 4.5: *Diffractogram obtained from XRD for crystals produced at 15 °C in run 1.7. The Y-axis represent the intensity of X-rays from the atoms, while the X-axis represents the diffraction angle.*

4.1.2.1 Key Findings: Cooling Crystallization - Mill 2

Findings from the experiments and analysis of run 1.6 to 1.10 will be presented in this section. It is based on the results that were disclosed during the first step of the recovery, where the bleed stream from Mill 2 was used to crystallize Product A. The most important findings are listed below.

- Cooling to 15 °C, rather than 25 or 32 °C, might produce more developed and pure crystals of Product A. An analysis of crystals obtained at other temperatures would, however, be required to prove this, for example, by XRD.

- It is not concluded that the efficiency is lower at 15 °C, compared to the other temperatures, as the calculations are potentially misleading.

- A slower cooling rate increased the yield of Product A and the potassium recovery efficiency.

- Product A crystallizes by itself from this bleed stream when being cooled in room temperature for up to 12 days.

- The IAP range of the bleed stream that allows crystallization of Product A has been identified and is presented in Figure 4.6.

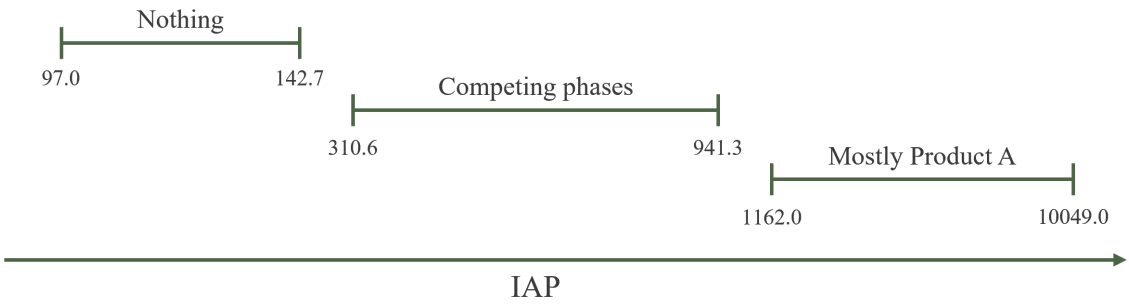

Figure 4.6: *IAP range of the bleed stream for the crystallization of Product A. The figure also illustrates the ranges where no crystallization occurred and where competing phases were formed.*

4.2 Results and Discussion: Step 2

This section will present the results and discuss the second step of the experimental phase where the goal was to re-crystallize Product B via the intermediate Product A. Only the screening test was conducted, according to the method in Section 3.2.6. Exact experimental measurements regarding for example specific weights and DS for all experimental runs can be seen in Appendix B.1 and Table B.1.

4.2.1 Re-crystallization to Product B via Intermediate Product A from Mill 1

Run 2.2 to 2.7 were performed with self-crystallized Product A from Mill 1. The leaching solution used in each run can be seen in Table 4.11. The amount of crystals that were dissolved during respective experiment is also displayed in the same table.

Table 4.11: *Dissolved crystals after conducted screening test for the second step with Product A from Mill 1.*

Run	Leaching Solution	Dissolved Product A [g, dry]
2.2	KCl sat. sol.	2.09
2.3	80/20 ML2 & water	9.17
2.4	50/50 ML2 & KCl sat. sol.	1.13*
2.5	50/30/20 ML2 & KCl sat. sol. & water	6.64*
2.6	90/10 ML2 & water	5.61
2.7	70/30 ML2 & water	11.83

*The dissolved amount was calculated without considering precipitated fine-textured solids.

In run 2.4 and 2.5 white fine-textured solids precipitated immediately after adding the reactants to the beaker, due to a reaction between ML2 and potassium chloride.

Therefore, the mass of these solids was not included when calculating the dissolved amount of Product A for those experiments. Apart from that, there were no major differences between the experiments. The amount of dissolved Product A, in dry mass, differed somewhat between the experiments. According to the reaction, and the theory in Section 2.2.2, Product A partly dissolves in aqueous potassium chloride, as the sodium-rich salt dissolves while the potassium-rich salt remains as crystals. Since run 2.7 had the highest water content and likely the lowest potassium concentration due to its dilution, and resulted in the greatest mass dissolution, this could suggest that some potassium was dissolved as well. To ensure that the potassium-rich salt does not dissolve, potassium should be in excess in the liquid.

The crystals from run 2.2 to 2.7 were analyzed using SEM-EDX, and a selection of the spectra is presented in Table 4.12. For all spectra, see Appendix B.2 and Table B.3. As mentioned, self-crystallized Product A from can SV was used for run 2.2 to 2.7, it will therefore be the reference point for the discussion regarding the result from the analysis. It can be seen in Table 4.12 that the chemical composition fluctuates between different locations within the samples, which makes it difficult to draw conclusions. Apart from a few exceptions, the concentration of potassium increased, and sodium decreased in the crystals from run 2.2 to 2.7, compared to the crystals from can SV. This indicates that some re-crystallization has occurred. The chemical composition of the powder that precipitated during run 2.4 and 2.5 implies that it is Product B. It was crystallized from free ions originating from the ML2 mimic and the solution saturated with potassium chloride. Furthermore, based on the concentration of sodium and potassium in the crystals, it is suggested that the re-crystallization was most effective for run 2.2, 2.4 and 2.5.

Table 4.12: *Selection of spectra of crystalline product after screening test with Product A from Mill 1. Index P denotes the fine-textured solids that precipitated during the run.*

Element [wt% dry mass]	**2.2**	**2.3**	**2.4**	**2.4$_P$**	**2.5**	**2.5$_P$**	**2.6**	**2.7**
Spectrum								
K	44.1	28.9	50.3	53.8	45.6	45.8	38.7	27.7
Na	1.67	9.4	0.3	0.1	0.2	0.1	6.1	11.3
C	0	5.2	1.3	4.4	1	0.3	1	3.3
O	34.3	38.1	28.7	20.8	34.7	19.1	33.6	37.9
S	18.3	18.1	19	20.8	18.3	19.1	20.5	19.7
Cl	1.7	0.2	0.5	0	0.2	0.1	0.6	0
Spectrum								
K	41.9	14.5	35.5	41.1	36.6	47.1	13	23.6
Na	2.1	13	8.7	0.1	6.6	0	22.3	13.2
C	0	20.5	0.3	0	1.5	0.3	1.8	4.3
O	36.4	37.8	33.2	41.2	34.7	33.2	44	40.8
S	18.1	14	22.2	17.5	20.4	19.4	18.5	18.1
Cl	1.4	0.2	0.1	0.1	0.2	0.1	0.4	0
Spectrum								
K	37.1	6	45.5	46.5	44.9	42.9	24.2	30.5
Na	7.6	26.6	0.4	0.1	0.5	0.1	13.5	7.8
C	0	2.5	1.3	1.1	0.3	0.4	2.3	7.8
O	34.1	43.8	34.2	32.9	35.4	38.6	40.6	40.9
S	21.2	20.9	17.9	19.2	18.2	18.1	19.3	18
Cl	0	0.2	0.7	0.2	0.7	0	0.1	0

The analysis of the potassium content in the liquids from run 2.2 to 2.7 is shown in Table 4.13. For all analysis data, see Appendix B.3 and Table B.5. That table shows that the sodium content has increased in ML2 for all experiments, compared to the leaching solution. Hence, it can be concluded that the sodium-rich salt has dissolved from the crystals. The potassium content has increased in ML2 for run 2.2, 2.3, 2.6, and 2.7, indicating that the potassium-rich salt has dissolved as well. A reaction may still have occurred where the potassium in the leaching solution reacted with the dissolved sodium-rich salt to form Product B. However, more potassium appears to have dissolved from the crystals than has re-crystallized. In run 2.4 and 2.5, the opposite trend was observed, where the potassium concentration in ML2 decreased, implying that re-crystallization dominated over dissolution. According to Table 4.13, run 2.4 showed the highest amount of potassium recovered to the crystals per dry Product A. These calculations are shown in Appendix B.4. The leaching solution used consisted of a 50/50 wt% mixture of a ML2 mimic and a saturated potassium chloride solution. This combination contains free potassium ions, which likely contributed to the formation of Product B. Additionally, Product A partly dissolved in the mixture, further promoting the formation of Product B

and resulting in a successful conversion. Conclusions made from the liquid analysis align with the ones made from the analysis with SEM-EDX.

Table 4.13: *Potassium analysis of the leaching solutions and ML2 from the second step, Mill 1. Where there is a negative value, potassium dissolved from Product A.*

Run	K in leaching solution [g]	K in ML2 [g]	Added Product A [g, dry]	K to/from solid phase [g K/(g dry Product A)]
2.2	2211.54	2311.29	20.01	-4.99
2.3	714.04	924.60	20.10	-10.48
2.4	1551.76	1171.46	20.01	19.01
2.5	1109.73	965.46	20.06	7.19
2.6	802.90	883.35	20.03	-4.01
2.7	624.62	904.90	20.01	-14.00

4.2.2 Re-crystallization to Product B via Intermediate Product A from Mill 2

Run 2.8 to 2.13 were performed with Product A from Mill 2 that was crystallized according to the method in Section 3.2.4. Table 4.14 shows which leaching solution that was used for respective experiments, along with the amount of dissolved crystals. Due to an experimental error, the solid content in all experiments for this screening test was 11.4 %.

Table 4.14: *Dissolved crystals after conducted screening test for the second step with Product A from Mill 2.*

Run	Leaching Solution	Dissolved Product A [g, dry]
2.8	KCl sat. sol.	3.53
2.9	80/20 ML2 & water	8.99
2.10	50/50 ML2 & KCl sat. sol.	-1.10
2.11	50/30/20 ML2 & KCl sat. sol. & water	4.78
2.12	90/10 ML2 & water	3.43
2.13	70/30 ML2 & water	8.82

The structure of Product A from Mill 2 differed significantly from that of Mill 1, appearing much finer in texture. Therefore, it was impossible to observe if any solids precipitated, as it did for two of the experiments using Product A from Mill 1. The corresponding experiments would be 2.10 and 2.11. However, it can be seen in Table 4.14 that the dissolved amount of crystals during run 2.10 was negative. It can therefore be assumed that solids did precipitate during that run as well, although it was not possible to separate it. The trend, where the highest mass of dissolved

crystals was found when using leaching solutions with the greatest water content, also holds true for these experiments.

Table 4.15 presents a selection of spectra obtained from the SEM-EDX analysis of the crystals obtained in run 2.8 to 2.13. For all spectra, see Appendix B.2 and Table B.4. Product A from run 1.7 at 15 °C was used in the re-crystallization and will be used as the reference point. Compared to crystals obtained from run 2.8 to 2.13, there is a difference in sodium and potassium content. The most significant differences are for run 2.8, 2.10 and 2.11, where the potassium content clearly has increased in the crystals and the sodium content has decreased. This is an indication of the desired re-crystallization.

Table 4.15: *Selection of spectra of crystalline product after screening test with Product A from Mill 2.*

Element [wt% dry mass]	**2.8**	**2.9**	**2.10**	**2.11**	**2.12**	**2.13**
Spectrum						
K	42.8	29.7	53.3	43.1	33.4	43.9
Na	1.2	7.9	0.2	1.2	7.6	5.2
C	0	1.2	0.5	1.0	1.0	0
O	35.1	43.9	25.1	35.5	38.7	27.8
S	16.3	17.2	20.5	17.6	19.2	23.1
Cl	4.6	0	0.5	1.6	0.1	0
Spectrum						
K	42.0	32.3	48.5	43.9	24.9	35.6
Na	1.9	9.1	1.8	1.1	13.5	7.0
C	0	4.1	0.3	0.5	1.2	0
O	33.2	34.2	26.8	35.4	40.6	37.8
S	15.2	20.3	18.7	18.2	19.6	19.7
Cl	7.6	0	4.0	0.8	0.2	0
Spectrum						
K	42.1	34.5	46.8	45.4	30.0	35.1
Na	0.9	8.5	0.2	0.3	10.8	7.7
C	0	1.3	0.6	1.0	0.7	0
O	37.1	34.7	32.8	34.3	39.0	37.4
S	17.2	20.9	19.4	18.8	19.5	19.8
Cl	2.6	0	0.3	0.2	0.1	0

In Table 4.16, the analysis of the potassium content in the liquids from run 2.8 to 2.13 are presented. All analysis data can be seen in Appendix B.3 and Table B.6, which shows that the sodium content has increased in ML2 for all experiments. The potassium content in ML2 has increased in run 2.9, 2.12 and 2.13, which indicates that dissolution of potassium was the predominant process over re-crystallization. For run 2.8, 2.10 and 2.11, the potassium content in ML2 has decreased according to the same trend as seen in run 2.4 and 2.5. Results from the SEM-EDX analysis

for the same experiments is consistent with this. Similar to the screening test using Product A from Mill 1, the same trends were observed regarding which leaching solution was most effective for re-crystallization. The same leaching solution was found to be the most effective for Mill 2, see run 2.10 in Table 4.16. In this screening test, the saturated solution of potassium chloride proved effective as well, with re-crystallization of potassium prevailing over dissolution. A hypothesis could be that the difference in the crystal structure of Product A affects the dissolution. The self-crystallized Product A may require more time, since the conversion efficiency is likely depending on the particle size.

Table 4.16: *Potassium analysis of the leaching solutions and ML2 from the second step, Mill 2. Where there is a negative value, potassium dissolved from Product A.*

Run	K in leaching solution [g]	K in ML2 [g]	Product A [g, dry]	K to/from solid phase [g K/(g dry Product A)]
2.8	2184.26	1999.00	22.81	8.12
2.9	664.16	824.04	22.85	-6.99
2.10	1507.79	1065.22	22.84	19.38
2.11	1070.30	930.89	22.86	6.10
2.12	747.09	792.36	22.82	-1.98
2.13	581.18	841.43	22.86	-11.38

Crystals from run 2.8 were also analyzed using XRD. The diffractograms from the analysis are presented in Figure 4.7, where the red in the peaks is an indication of a certain phase found in the sample. This analysis showed that three phases were present: Product B, Product A and potassium chloride. Based on the analysis, the sample mostly contained Product B, see Figure 4.7a, and it can be concluded that the re-crystallization was partly successful for this experiment. There were some remaining Product A, see Figure 4.7b, that was not re-crystallized during the experiment. It can not be established whether this was due to insufficient time or if a different solid concentration was required. The potassium chloride that was found in the sample, see Figure 4.7c, most likely came from the saturated solution. Based on this result, along with other findings, it is assumed that all experiments in the screening test achieved some degree of re-crystallization of Product B. However, the efficiency of this conversion can not be determined without further analysis.

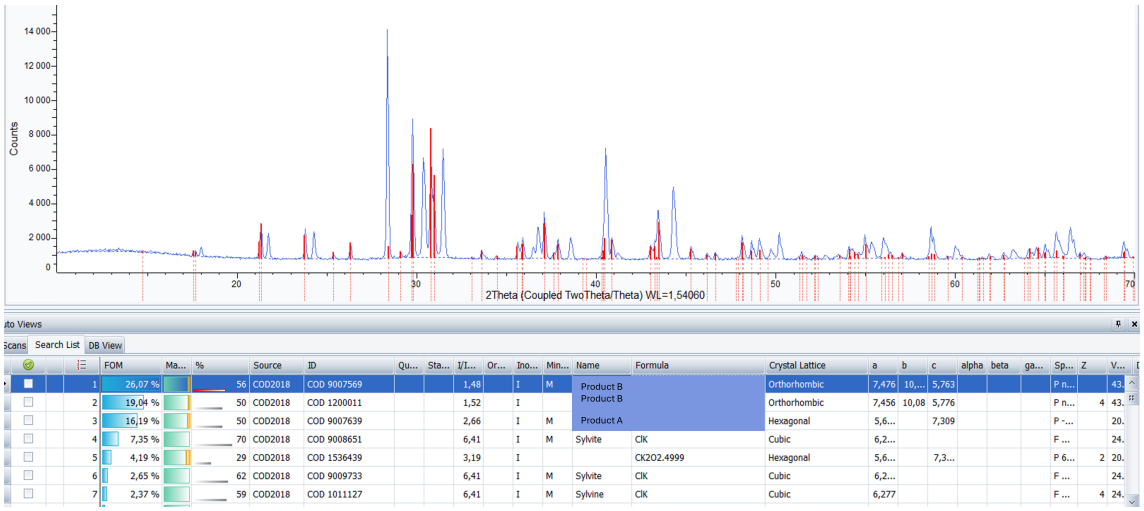

(a) *Diffractogram of the Product B phase for run 2.8.*

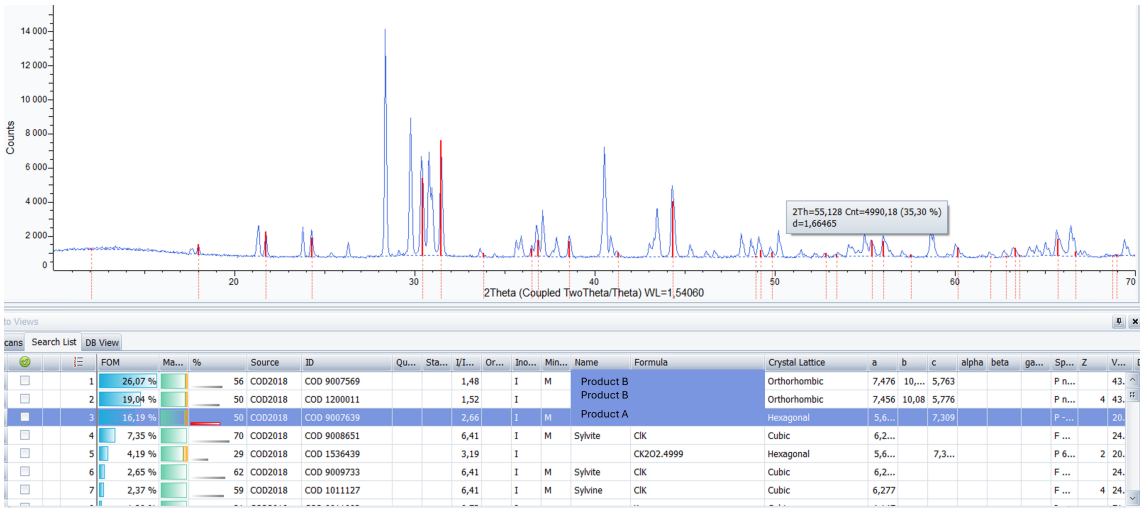

(b) *Diffractogram of the Product A phase for run 2.8.*

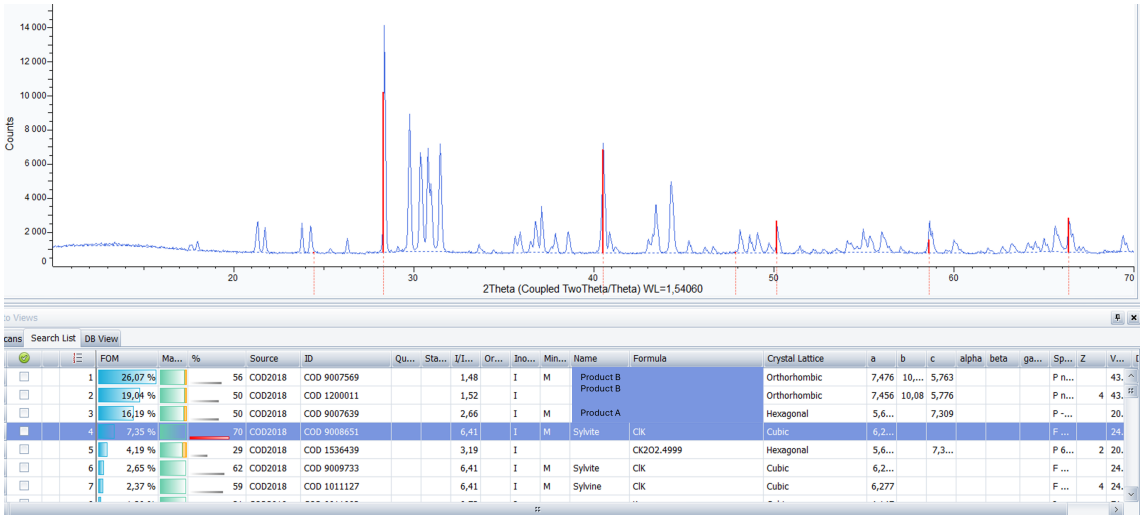

(c) *Diffractogram of the potassium chloride phase for run 2.8.*

Figure 4.7: *Diffractograms for the different phases in the product obtained from run 2.8. The Y-axis represent the intensity of X-rays from the atoms, while the X-axis represents the diffraction angle.*

Figure 4.8 displays an image of the product obtained in run 2.8, which was confirmed to be mostly Product B. There is a distinct difference in appearance compared to the starting material, see Figure 4.4a. The change in crystal morphology primarily involves the crystal shape, as Product A appeared hexagonally, whereas Product B from run 2.8 does not.

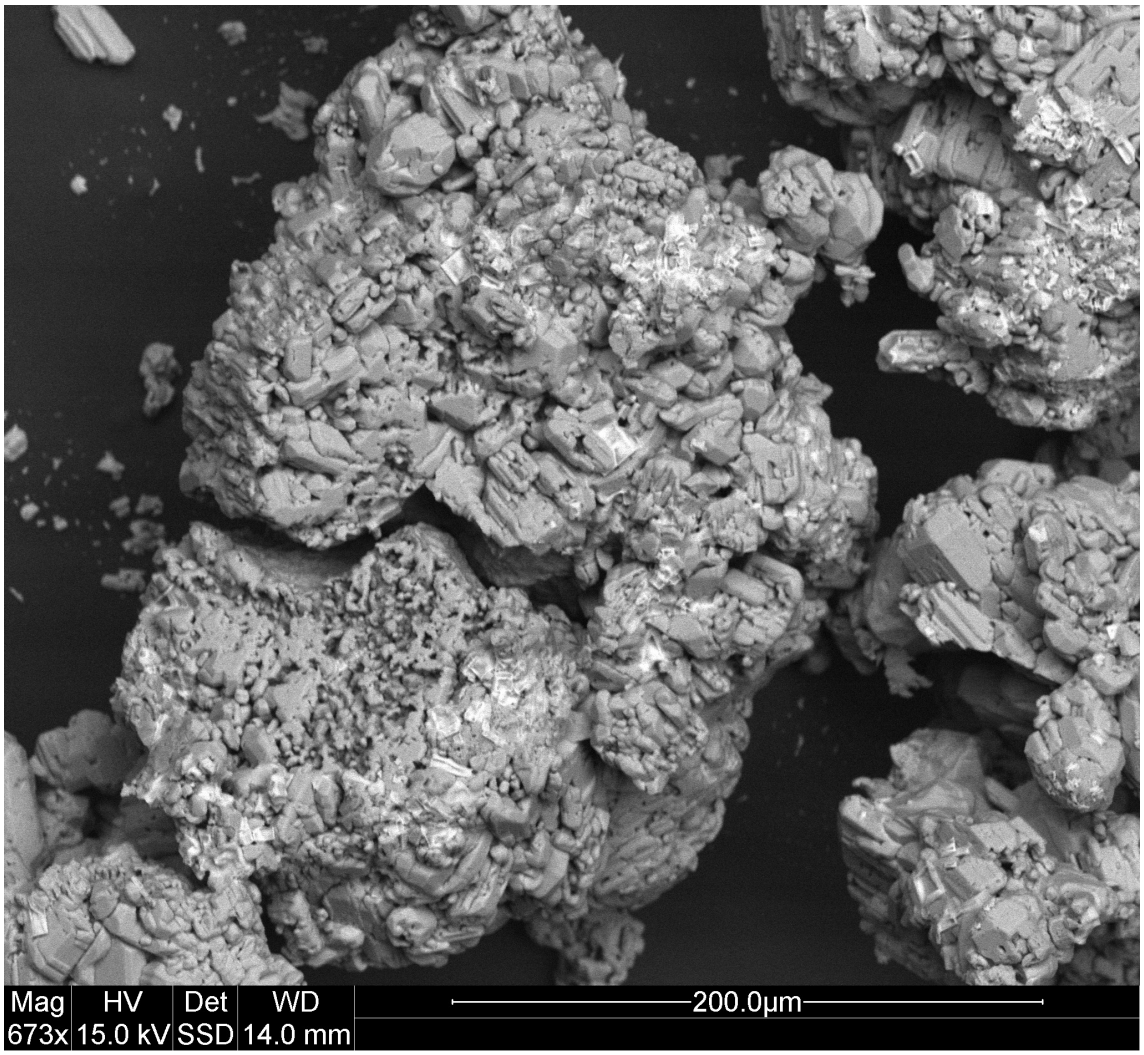

Figure 4.8: *Image obtained through SEM of the crystals from run 2.8, confirmed to be partly Product B through XRD.*

Figure 4.9 provides a side-by-side comparison of crystals that were obtained over the course of this project. From left to right, the figure displays: Crystals from run 1.3, self-crystallized Product A from can SV, Product A from run 1.7 at 25 °C and Product B from run 2.8.

Figure 4.9: *From left to right, crystals obtained from run 1.3, can SV, run 1.7 and run 2.8*

4.2.3 Key Findings: Re-Crystallization

Findings from the experiments and analyses of run 2.2 to 2.13 will be presented in this section. They are based on the results that were revealed during the second step of the experimental phase, where the intermediate Product A was used for the re-crystallization to Product B. The most important findings are listed below.

- The liquid found to be most effective for the conversion of Product B from Product A was a 50/50 wt% mixture with a ML2 mimic and a saturated solution with potassium chloride. This finding was consistent for both Mill 1 and Mill 2.
- Based on the elemental analysis on liquid and solid phases, the conversion was successful for all liquids. However, it is not possible to know to which extent without further research.
- When leaching solutions only containing ML2 and water are used, conversion to Product B seems to be based on dominant dissolution of the sodium-rich salt and only partial dissolution of the potassium-rich salt.
- When potassium chloride is added to the leaching solution there is not only dissolution, but also re-crystallization from free ions taking place.

4.3 Evaluation of Energy Demand and Process Comparison

The energy evaluation for the cooling crystallization was simulated and calculated with MATLAB, according to the method in Section 3.3. The code that was used is presented in Appendix C.1. The energy required to cool the bleed stream from the starting temperature to the target temperature was calculated for run 1.1, 1.5,

1.9 and 1.10. These experiments were chosen to determine the difference in energy demand for the two mills when slow and fast cooling is applied. The calculations can also give an estimation of the difference in energy use between the conventional production of Product B and the new process tested in this report. Since the experiments with bleed stream from Mill 1 did not obtain the desired Product A, run 1.1 and 1.5 will not be included in the comparison of energy demand with the conventional process.

For Mill 1, the energy demand for fast cooling, conducted in run 1.1, was 1611.81 kJ, while it was 3973.25 kJ for slower cooling, conducted in run 1.5. However, since not exactly the same amount of product was produced in these runs, the energy demand was re-calculated with that taken into account. The energy demand for run 1.1 and 1.5 was therefore 6.68 kJ/(g Product C) and 2.66 kJ/(g Product C), respectively. Since the crystals obtained from these runs contained multiple undesired phases, they will be referred to as Product C. These results show that the energy demand for the fast cooling is more than double the one for the slow cooling. For Mill 2, the energy demand for run 1.9, slow cooling, was 2209.0 kJ, whereas for run 1.10, fast cooling, it was 2458.7 kJ. When the dry mass of Product A was taken into consideration, it was re-calculated to 5.84 kJ/(g dry Product A) and 10.39 kJ/(g dry Product A), for run 1.9 and 1.10 respectively. Again, the energy demand for fast cooling is thus nearly doubled compared to the slow cooling. From a process design perspective, these findings suggest that slower cooling could offer substantial energy savings, and improved efficiency as indicated in Section 4.1.1. Slower cooling could also have a positive impact on the crystal morphology and purity. The trade-off, however, may include longer cycle times and a lower hourly production which results in reduced revenue. This would need to be evaluated in a broader optimization context. Figures 4.10 and 4.11 show $T_{reactor}$ over time for run 1.1 and run 1.5, respectively. Figure 4.11 displays an increase in the temperature at just above 20 °C, which can be an indication that an exothermic crystallization started at this temperature. This reaction is not seen in Figure 4.10, where the cooling supply constantly exceeded the demand.

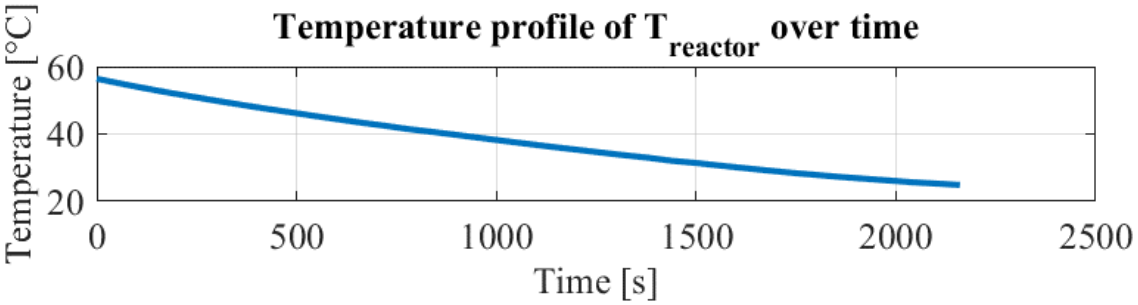

Figure 4.10: *The graphs present the temperature profile of $T_{reactor}$ over time for run 1.1.*

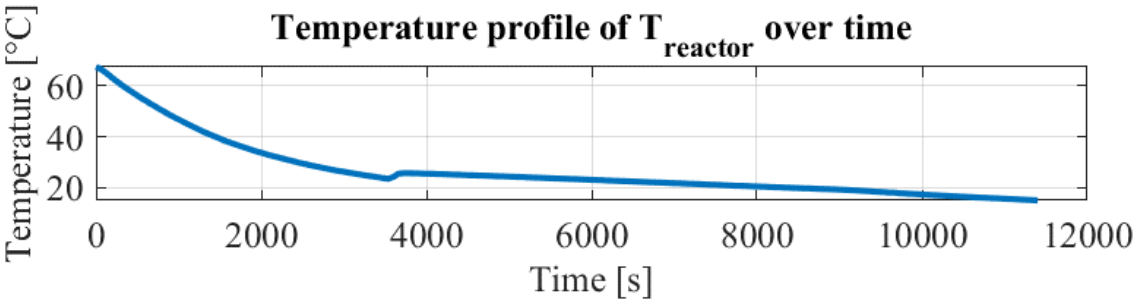

Figure 4.11: *The graphs present the temperature profile of $T_{reactor}$ over time for run 1.5.*

Table 4.17 presents the energy demands, per dry mass Product B, for the conventional production, run 1.9 and 1.10. Since it is not known how much Product B would have been obtained from run 1.9 and 1.10, an estimation has been made. Results from run 2.4 were used to calculate the amount of Product B obtained based on the quantity of Product A used. This run was chosen since the leaching solution used was deemed the most effective for re-crystallization of Product A into Product B. Furthermore, results from run 2.12 were also used for the calculations, as this run had the most effective conversion with a leaching solution that did not contain any additional chemicals. For the calculations it has been assumed that the product from the chosen experiment was purely Product B, which is very unlikely. The energy demand for run 1.9 and 1.10 will therefore be presented with the unit kJ/(g dry Product B_{dirty}). Relevant calculations can be seen in Appendix C.2. It can be seen from Table 4.17 that the energy demand for the new process is lower than for the conventional process, not the least when slow cooling is applied. Best conversion efficiency of Product A to Product B is achieved when using the same leaching solution as in run 2.4. However, by implementing the leaching solution used in run 2.12, it results in a lower cost for the plant as no additional chemicals are needed.

Table 4.17: *Comparison of energy demand between the conventional process and the new process tested in this report, with slow and fast cooling applied.*

Process	**Energy demand [kJ/(g dry Product B)]**
Conventional	15.6
Run $1.9_{2.4}$	6.21*
Run $1.9_{2.12}$	8.04*
Run $1.10_{2.4}$	11.05*
Run $1.10_{2.12}$	14.31*

*[kJ/(dry Product B_{dirty})]

An advantage of the new process for producing Product B, compared to the conventional method, is the difference in the by-product formed. For the conventional process, the by-product is the highly dangerous hydrochloric acid, which in gaseous

form is extremely toxic. However, for the new process tested in this project, the by-product is an aqueous salt solution containing relatively low-toxicity ions. Thus, the new process is safer to operate. The maximum temperature that the new process reaches is 80-100 °C, since it is the temperature of the bleed stream when purged from the mill. These temperatures are considered very moderate compared to 600 °C, which is the temperature at which the conventional production of Product B operates. Not only is it more dangerous working at such elevated temperatures, it also puts a lot more strain on the equipment. This results in higher investment costs, and/or more maintenance. Increased maintenance would entail higher costs and more downtime. The new process is therefore considered to be more cost-effective in that regard. Furthermore, it only utilizes cooling, if no further treatment of the mother liquors is made. Cooling mediums are generally less expensive compared to heating mediums. Moreover, if the site is strategically located, an existing body of water could be utilized for cooling purposes.

4.4 Methodological Challenges and Process Variability

The method for crystallization was generally effective, but there were a few details that created inconsistencies between the experiments. Firstly, the heating cabinet that was used was not very effective. The bleed stream rarely reached the targeted temperature, unless it was further heated. The starting temperature before cooling therefore fluctuated a bit between the experiments. Furthermore, it might have been possible to dissolve the solids, found in the cans from Mill 1, if the heating cabinet would have been a more effective heating source. The time that the bleed stream was kept in the heating cabinet before being used also differed significantly between each experiment, since there was no set schedule for this. Considering that more time in heat results in more dissolution, this can make a profound difference in the results. This would not have been an issue if the solids had easily re-dissolved in the bleed stream. However, the composition of the bleed stream likely changed depending on the time spent in the heating cabinet. Therefore, it is important to measure the DS of the bleed stream before conducting every experiment, though this was unintentionally missed a few times. Further, it was difficult to control the cooling rate. Although the same settings were used for the cooling machine, the cooling rate fluctuated a lot between the experiments. This depended on the target temperature, the mass of bleed stream, and its starting temperature, which made it hard to achieve a specific cooling rate. Furthermore, the formation of different solids requires different amounts of energy.

4.4.1 Limitations and Reliability of Analytical Methods

The main method used for solid analysis throughout the project was SEM-EDX, which is an effective tool for analyzing the elemental composition of crystals. However, since the crystals obtained from most experiments, mainly when using the bleed stream from Mill 1, were a mixture of multiple salts, it was difficult to assess the

quantity of these salts with SEM-EDX. This may lead to some misunderstandings regarding the results. During analysis, specific locations were deliberately chosen to show the presence of multiple phases. This might give the impression that there were more locations, within the sample, with a low potassium content when in fact it may not be true. Furthermore, some of the crystals were dried before being analyzed with the SEM-EDX. This is because they were too wet to be analyzed with high vacuum. This generated results that were not fully reliable. When drying wet samples, it is not possible to determine whether crystallization occurred during the experiment or the drying process. Dissolved salts in trapped mother liquor would be crystallized during the drying. XRD proved to be a more effective method for quantifying and identifying the present phases in a sample. This analysis method could unfortunately only be used on two samples, due to unavailability.

The method used for liquid analysis was ICP-AES. This was generally a good method for the purpose. For the second step, three different saturated liquids were prepared, these were made at room temperature and filtered to remove excess solids. Even though the liquids were stored at room temperature when transported to the commercial laboratory, where they were analyzed, the temperature might have fluctuated. There had been some precipitation in one of the liquids upon arrival, so the results of that analysis will consequently present a different chemical composition compared to when it was used. To ensure more accurate results, it would have been preferable if the analyses could have been performed shortly after taking the samples, but this was not possible. Furthermore, since the liquids are sent to a commercial laboratory, errors such as unrealistic results will not be detected during the analysis. This could have been mitigated if the analysis had been performed in-house.

5
Conclusion

This chapter will present the conclusions that can be drawn from the project and provides suggestions on improvements and further research of the process.

The cooling crystallization method for the formation of Product A from a bleed stream, which is purged after the ash treatment in a pulp mill, is viable. The obtained crystals of Product A are pure and well-formed, as seen in analysis from XRD and SEM-EDX. However, it is a sensitive process, as it highly relies on the composition of the bleed stream. It has been observed that it is necessary for the bleed stream to have a high IAP with regard to Product A. For conducted experiments, Product A crystallized in the range of 1162.0-10049.0. Outside of this range, competing phases were formed or crystallization did not occur at all.

Slow cooling has been identified as an important factor for this method. It has been shown to affect the potassium recovery efficiency and the yield of Product A. It has been confirmed that the method together with a slow cooling rate, obtains more developed, purer and well-formed crystals. The most developed crystals were retrieved at 15 °C, as demonstrated in run 1.7. This may be due to the low final temperature, but also to the fact that the cooling rate decreases naturally as it approaches the target temperature. Furthermore, slow cooling seems to favor the formation of Product A before competing phases, and is therefore recommended.

The re-crystallization method for the conversion to Product B via the intermediate Product A is also proved to be viable. Diffractograms for run 2.8 indicated that Product B was the predominant phase in the re-crystallized product. It is assumed that all experiments in the screening test underwent some level of conversion, as supported by both liquid and solid phase analyses. The leaching solution found to be most effective for both mills in promoting this conversion during the screening test was a 50/50 wt% mixture of a ML2 mimic and a saturated potassium chloride solution.

When compared to the conventional process of Product B, the new process is less energy demanding, both for slow and fast cooling crystallization. The new process is also less dangerous with regards to the by-product and operational parameters. The results from the second step of the experimental phase suggest that a mixture with ML2 can effectively promote the conversion of Product A to Product B, thereby enhancing the feasibility of recycling ML2 within the process. This will further benefit the new process, as recirculation is generally preferred due to its potential to

enhance resource efficiency and increase overall yield.

In conclusion, the methods of cooling crystallization and re-crystallization show potential to be implemented in an ash treatment process to enhance the circularity and sustainability of the pulp mill and return lost nutrients to the trees through the commercial Product B. Implementing such a process could also aid with improving the general image of the company and comply with potential future regulations on what goes to effluent treatment. However, there is a need for further optimization and process development to determine if the process is technically and economically feasible on a larger scale.

5.1 Suggestions for Improvement and Further Research

Once a process is found to be technically operable, the next consideration is its economic feasibility, since this often becomes the deciding factor in whether the process is ultimately implemented. The profit from a potential implementation has not been evaluated in this project, and would therefore be a natural next step for further research. Income from selling Product B could be compared to the investment and operational costs for equipment and consumables, and the payback period could be calculated to assess the economic viability. The most effective leaching solution, without the addition of chemicals, was a 90/10 wt% mixture of ML2 and water. It would be valuable to investigate the trade-off between a decreased conversion efficiency and the cost savings from not purchasing additional chemicals.

The initial focus of the project was to optimize the method for recovering potassium from a purge stream originating from an ash treatment process, with the goal of improving yield and facilitating the conversion into a commercial product. Given that the method has been proven to be applicable, it would be valuable for further research to revisit the initial focus on optimization. For example, further investigating the effects of cooling rate for the first step of potassium recovery. This was attempted for run 1.9 and 1.10, where both slow and fast cooling rates were applied. However, controlling this proved difficult, and there was not a very big difference between the two experiments. Nevertheless, run 1.9 yielded noticeably more crystals. Since the optimal cooling rate for the formation of Product A, as reported in the literature, is 0.2 °C/min, it would have been valuable to apply this rate to assess whether it could have resulted in an even higher yield, given that the cooling rate in Run 1.9 was significantly higher. Regarding the second step of potassium recovery, it is of interest to investigate whether the incomplete re-crystallization of Product B from Product A is due to, for example, insufficient residence time or to an incompatible solid concentration.

Lastly, since XRD was assessed to be a better alternative to determine the phases within a sample, when there are multiple samples, it should have been used for all samples if this project were to be redone. ICP-AES of dissolved crystals could also be preferable, to provide actual potassium, sodium and sulfate concentrations.

Bibliography

1. Arias A, Feijoo G, and Moreira MT. Biorefineries as a driver for sustainability: Key aspects, actual development and future prospects. Tech. rep. Santiago de Compostela, Spain: Department of Chemical Engineering, School of Engineering, University of Santiago de Compostela, 2023. DOI: 10.1016/j.jclepro.2023.137925
2. Munawar MA and et. al. Challenges and opportunities in biomass ash management and its utilization in novel applications. Tech. rep. Islamabad, Pakistan: Department of Thermal Energy Engineering, U.S.-Pakistan Centre for Advanced Studies in Energy, 2021. DOI: 10.1016/j.rser.2021.111451
3. Cheng F and Brewer C. Producing jet fuel from biomass lignin: Potential pathways to alkylbenzenes and cycloalkanes. Tech. rep. Las Cruces: Department of Chemical and Materials Engineering, New Mexico State University, 2017
4. Rajan K, Berton P, Rogers R, and Shamshina J. Is Kraft Pulping the Future of Biorefineries? A Perspective on the Sustainability of Lignocellulosic Product Development. Polymers 2024; 16(23). DOI: https://doi.org/10.3390/polym16233438
5. Winberg K. Mass balances of carbonate and oxalate in a Kraft pulp mill. Tech. rep. Gothenburg, Sweden: Chalmers University of Technology and Stora Enso, 2015. Available from: https://publications.lib.chalmers.se/records/fulltext/221123/221123.pdf
6. Gupta A and Kulkarni A. Non-Process Elements in Agro Based Black Liquors And Their Influence On Chemical Recovery Operations. Central Pulp Paper Research Institute, 1997 :91–8. Available from: https://ippta.co/wp-content/uploads/2021/01/IPPTA-93-91-98-Non-Process-Elements.pdf
7. Neri A, Cagno E, and Trianni A. Barriers and drivers for the adoption of industrial sustainability measures in European SMEs: Empirical evidence from chemical and metalworking sectors. Sustainable Production and Consumption 2021; 28:1433–64. DOI: https://doi.org/10.1016/j.spc.2021.08.018
8. European Commission, Luiza. Wastewater regulations for European industrial dischargers 2025. Accessed: 2025-04-24. 2025. Available from: https://aquacycl.com/blog/wastewater-regulations-for-european-industrial-dischargers-2025/

9. Hacker J. Effects of Logging Residue Removal on Forest Sites. Tech. rep. Eau Claire, Wisconsin: West Central Wisconsin Regional Planning Commission, 2005. Available from: https://dnr.wisconsin.gov/sites/default/files/topic/ForestBusinesses/LoggingResidueReport.pdf

10. Dimian A, Bildea C, and Kiss A. Chapter 11 - Batch Processes. *Integrated Design and Simulation of Chemical Processes*. Ed. by Dimian A, Bildea C, and Kiss A. Vol. 35. Computer Aided Chemical Engineering. Elsevier, 2014 :449–88. DOI: https://doi.org/10.1016/B978-0-444-62700-1.00011-5. Available from: https://www.sciencedirect.com/science/article/pii/B9780444627001000115

11. AQION. Mineral Solubility and Saturation Index. Accessed: 2025-05-09. 2025. Available from: https://www.aqion.de/site/168

12. Richardson J, Harker J, and Backhurst J. Crystallisation. *Chemical Engineering (Fifth Edition)*. Ed. by Richardson J, Harker J, and Backhurst J. Fifth Edition. Chemical Engineering Series. Oxford: Butterworth-Heinemann, 2002 :827–900. DOI: https://doi.org/10.1016/B978-0-08-049064-9.50026-6. Available from: https://www.sciencedirect.com/science/article/pii/B9780080490649500266

13. Svarovsky L. Solid-Liquid-Separation. Ed. by Svarovsky L. 4th. Oxford: Butterworth-Heinemann, 2000. Available from: https://himatekkim.ulm.ac.id/id/wp-content/uploads/2021/06/Svarovsky-L-%E2%80%93-Solid-Liquid-Separation-4th-Edition.pdf

14. Mubarak Y. Integrated process for potassium sulfate and a mixture Of ammonium chloride/potassium sulfate salts production. International Journal of Engineering Technology 2018; 7:185–97. DOI: 10.14419/ijet.v7i1.9188. Available from: www.sciencepubco.com/index.php/IJET

15. Grzmil BU and Kic B. Single-Stage Process for Manufacturing of Potassium Sulphate from Sodium Sulphate. Tech. rep. PL-70 322. Szczecin: Technical University of Szczecin, 2005

16. Liedberg J. Process for production of a fertilizer comprising potassium sulfate. FI128696B. AB AE. Finland of patent. 2020

17. Garret D. Potash: Deposits, processing, properties and uses. Chapman and Hall, 1996 :440–92. DOI: 10.1007/978-94-009-1545-9. Available from: https://link.springer.com/chapter/10.1007/978-94-009-1545-9_7

18. Khlissa F, M'nif A, and Rokbani R. Application of the conductimetry to the study of the transformation of KCl and Na2SO4 into K2SO4 between 5 and 30 ◦ degree C. Tech. rep. B.P. 95-2050, Hammam-Lif, Tunisia: Institut National de Recherche Scientifique et Technique, 2003

19. Bessenet S, Feng J, Rieke J, and Rittoe T. METHODS FOR PRODUCING POTASSIUM SULFATE AND SODIUM CHLORIDE FROM WASTEWATER. BR112019011795. INC VWT. Brittain of patent. 2023

20. Antonova N, Naginskaya R, Ostanina V, Rutkovskaya T, Safrygin J, Sokolov I, and Naginskaya R. Method of producing potassium sulfate. US4215100. Antonova N, Naginskaya R, Ostanina V, Rutkovskaya T, Safrygin J, Sokolov I, and Naginskaya R. United States of patent. 1980

21. Holdengraber C and Lampert S. Process for producing potassium sulfate from potash and sodium sulfate. US6143271. WORKS DS. United States of patent. 2000

22. Mazzarotta B. Crystallization of glaserite from aqueous solutions. *Crystal Research and Technology*. Vol. 25. Wiley, 1990 :903–11. DOI: https://doi.org/10.1002/crat.2170250810. Available from: https://onlinelibrary.wiley.com/doi/10.1002/crat.2170250810

23. Soliev L and Tursunbadalov S. Phase Equilibria in the Na, K//SO4, CO3, HCO3 – H2O System at 50C. Teesside, UK: Materials Science and Engineering, 2013. DOI: 10.1088/1757-899X/47/1/012050

24. Shi B and Rousseau R. Structure of Burkeite and a New Crystalline Species Obtained from Solutions of SodiumCarbonate and Sodium Sulfate. Atlanta, Georgia: School of Chemical Engineering, Georgia Institute of Technolog, 2003. DOI: 10.1021/jp0277053

25. Education Open Textbook Pilot Project D of. Reaction Yields. Accessed: 2025-03-04. Available from: https://chem.libretexts.org/Bookshelves/General_Chemistry/Chemistry_1e_(OpenSTAX)/04%3A_Stoichiometry_of_Chemical_Reactions/4.05%3A_Reaction_Yields

26. Johnson M, Heggs P, and Mahmud T. An assessment of OHTC models to predict the performance of laboratory-scale jacketed batch reactors. Organic Process Research Development 2016; 20:204–14. DOI: 10.1021/acs.oprd.5b00378

27. Shahvarooghi F, Zamanifard H, and Taki M. Assessing the energy load and environmental footprint of potash fertilizer production in Iran. PLoS One 2024 Nov. DOI: 10.1371/journal.pone.0313129

28. Artioli G. X-ray Diffraction (XRD). *Encyclopedia of Geoarchaeology*. Ed. by Gilbert AS. Dordrecht: Springer Netherlands, 2017 :1019–25. DOI: 10.1007/978-1-4020-4409-0_29. Available from: https://doi.org/10.1007/978-1-4020-4409-0_29

29. Askeland D. The Science and Engineering of Materials. 6th ed. Cengage Learning, 2010. Available from: https://anupturnedworld.wordpress.com/wp-content/uploads/2016/06/askeland-the-science-and-engineering-of-materials.pdf

30. Persdotter A and Ssenteza V. Labbmanual för Mikroskopi-labb: Svepelelektronmikroskopi (SEM) och Röntgendiffraktion (XRD). Course page, available for students registered on the course. 2023

31. Harvey D. Modern Analytical Chemistry. 2.1. McGraw-Hill Companies, 2016. Available from: http://dpuadweb.depauw.edu/harvey_web/eTextProject/AC2.1Files/AnalChem2.1.pdf

32. College W. Chapter 4: Inductively Coupled Plasma—Atomic Emission Spectrometry. Withman College, 2017. Chap. 4. Available from: https://www.whitman.edu/chemistry/edusolns_software/FAAS_ICP_2017/CH4_ICP-AES_2017.pdf

33. Nation E. Water-glycol Calculate the properties of water - ethylene glycol mixture. Accessed: 2025-03-10. 2020. Available from: https://engineeringnation.com/water-glycol/

A

Appendix

This appendix presents information about the first experimental phase of the project; crystallization of Product A.

A.1 Step 1: Detailed experimental measurements

Table A.1 presents detailed information about the experiments in the first step regarding masses and DS for the bleed stream, ML1 and obtained crystals. It also presents the dry mass for each component. The table includes experiments made with bleed stream from Mill 1 and Mill 2.

Table A.1: *Detailed experimental measurements for experimental runs of the first step. DS is an average for the crystals. Where no data is stated, no crystals were formed.*

	Mass [g]	**DS [%]**	**Mass [g, dry]**
Run 1.1			
Bleed	6827	31.2	2130.0
ML	6143	29.5	1812.2
Crystals	582.7	42.2	245.9
Run 1.2			
Bleed	6711	31.2	2093.8
ML 1^{st} filtr.	2041	29.7	606.2
ML 2^{nd} filtr.	344	27.8	95.6
ML 3^{rd} filtr.	2425	22.5	545.6
Crystals 1^{st} filtr.	—	—	—
Crystals 2^{nd} filtr.	73	39.2	28.6
Crystals 3^{rd} filtr.	1582	41.02	648.9
Run 1.3			
Bleed	6835	33.5	2289.7
ML	3651	24.3	887.2
Crystals	2787	43.0	1198.4
Run 1.4			
Bleed	4663	32.2	1501.5
ML	3416	29.2	997.5

(Continued on next page)

Table A.1 – continued from previous page

	Mass [g]	DS [%]	Mass [g, dry]
Crystals	1046	42.4	443.5
Run 1.5			
Bleed	7020	31.5	2211.3
ML	3427	23.1	791.6
Crystals	3336	44.8	1494.5
Run 1.6			
Bleed	6494	28.7	1863.8
ML	—	—	—
Crystals	—	—	—
Run 1.7			
Bleed	6622	31.0	2052.8
ML 1^{st} filtr.	215.5	27.3	58.8
ML 2^{nd} filtr.	385	25.2	97.0
ML 3^{rd} filtr.	5593	29.1	1627.6
Crystals 1^{st} filtr.	24.6	85.6	21.1
Crystals 2^{nd} filtr.	43.8	85.9	37.6
Crystals 3^{rd} filtr.	146	95.7	139.7
Run 1.8			
Bleed	6402	29.1	1863.0
ML	—	—	—
Crystals	—	—	—
Run 1.9			
Bleed	6812	33.3	2268.4
ML	6324	27.4	1732.8
Crystals	451	83.9	378.4
Run 1.10			
Bleed	6622	32.2	2132.3
ML	6295	28.6	1800.4
Crystals	260.5	90.9	236.8

A.2 Step 1: Images from Cooling Crystallization

This section presents images from the first step of the experimental phase. The intention is to give a better understanding of the experiment and explanations given in the result and discussion section. Figure A.1 shows the funnel after filtration of run 1.1. The funnel is filled with large crystals to the brim. These crystals are not Product A, but rather a competing phase. Figure A.2 illustrates that the funnel remains less than half full after the filtration of run 1.9, and the crystals are much smaller compared to the others. These crystals are Product A.

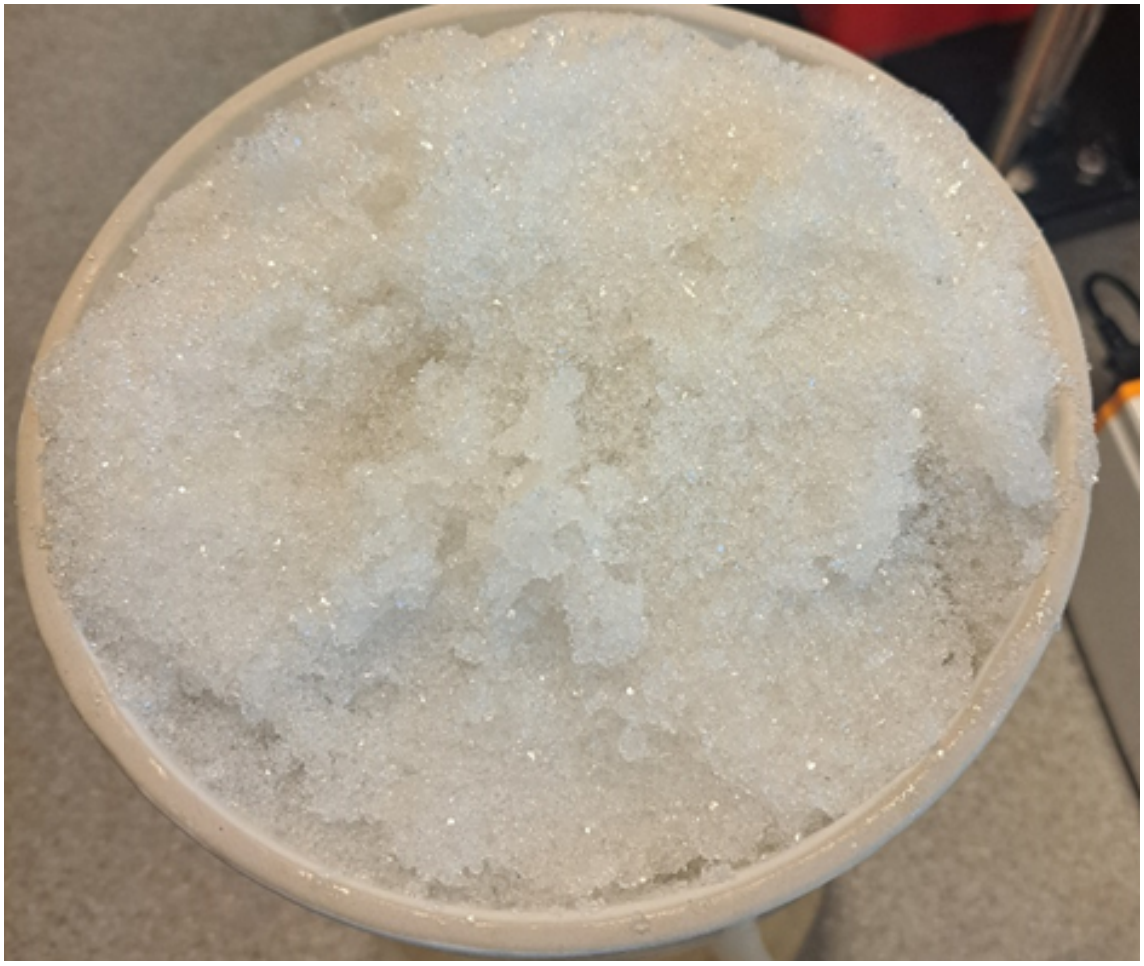

Figure A.1: *Full funnel with crystals after filtration of run 1.1, bleed stream from Mill 1.*

Figure A.2: *Funnel with crystals after filtration of run 1.9, bleed stream from Mill 2.*

A.3 Step 1: Results from Solid Analysis

This section presents the solid analyses performed using SEM-EDX during the first step of the experimental phase. Table A.2 shows the spectra of the crystal compositions from run 1.1 to 1.5, while Table A.3 displays the spectra of the solids collected from the cans with bleed stream from Mill 1 and Mill 2. The last table, Table A.4 presents all the spectra of the compositions of crystals obtained from run 1.6 to 1.10.

Table A.2: *All spectra for obtained crystals in experiment using bleed stream from Mill 1.*

Element [wt% dry mass]	1.1*	1.2*	1.3	1.4	1.5*
Spectrum					
K	1.9	0	1.1	2.1	0
Na	31.2	18.1	31.2	33.9	31.8
C	4.5	20.5	4.1	0	3.6
O	43.3	34	42.6	44.2	44.2
S	16.9	27.3	19.4	18.6	20.4
Cl	2.2	0	1.3	1.1	0
Spectrum					
K	1.8	1.1	31.6	25.4	0
Na	33.2	28.5	8.4	12.7	30.6
C	0	10.2	4.1	2.9	0
O	42.7	43.6	37.4	41.9	42.7
S	19.9	15.9	18.6	16	26.8
Cl	2.4	0.7	0	1.1	0
Spectrum					
K	1.2	0.8	28.3	—	0
Na	33.6	31.8	10.2	—	33.4
C	0	0	5.8	—	0
O	43.3	44.1	37.6	—	44.6
S	19.2	23.2	18.1	—	21.9
Cl	2.8	0	0	—	0
Spectrum					
K	0.4	0	—	—	24.8
Na	29.4	29.6	—	—	15.3
C	4.2	8.0	—	—	0
O	42.7	43.3	—	—	42
S	22.9	19.1	—	—	18
Cl	0.4	0	—	—	0
Spectrum					
K	1.2	0	—	—	22.4
Na	30.5	30.3	—	—	16.5
C	5.5	0	—	—	0
O	41.9	41.5	—	—	43.4
S	20	28.2	—	—	17.7
Cl	0.9	0	—	—	0
Spectrum					
K	1.2	1.1	—	—	0

(Continued on next page)

Table A.2 – continued from previous page

Element [wt% dry mass]	1.1*	1.2*	1.3	1.4	1.5*
Na	33.5	29.3	—	—	29.4
C	4.7	5.8	—	—	4.9
O	41.3	41	—	—	41
S	15.8	18.9	—	—	24.8
Cl	3.5	3.9	—	—	0
Spectrum					
K	—	0	—	—	0.4
Na	—	31.2	—	—	29.8
C	—	3.5	—	—	5.2
O	—	42.7	—	—	41.1
S	—	22.6	—	—	22.6
Cl	—	0	—	—	0.9
Spectrum					
K	—	0	—	—	0
Na	—	31.2	—	—	27.4
C	—	3.5	—	—	12.7
O	—	43.1	—	—	41
S	—	22.2	—	—	18.9
Cl	—	0	—	—	0
Spectrum					
K	—	0.5	—	—	0
Na	—	32.7	—	—	33.9
C	—	0	—	—	0
O	—	41.1	—	—	44.5
S	—	22.4	—	—	21.6
Cl	—	3.3	—	—	0
Spectrum					
K	—	—	—	—	1.5
Na	—	—	—	—	30.4
C	—	—	—	—	8
O	—	—	—	—	42
S	—	—	—	—	17.2
Cl	—	—	—	—	0.9
Spectrum					
K	—	—	—	—	23
Na	—	—	—	—	13.7
C	—	—	—	—	8.1
O	—	—	—	—	36.3
S	—	—	—	—	17.4
Cl	—	—	—	—	1.5

(Continued on next page)

Table A.2 – continued from previous page

Element [wt% dry mass]	1.1*	1.2*	1.3	1.4	1.5*
Spectrum					
K	—	—	—	—	0.2
Na	—	—	—	—	23.9
C	—	—	—	—	18.5
O	—	—	—	—	39.7
S	—	—	—	—	16.6
Cl	—	—	—	—	1.1
Spectrum					
K	—	—	—	—	0
Na	—	—	—	—	22.8
C	—	—	—	—	16.1
O	—	—	—	—	38.9
S	—	—	—	—	20.9
Cl	—	—	—	—	1.3

*The samples were dried before being analyzed with the SEM-EDX.

Table A.3: *All spectra for solids found in cans of bleed stream from Mill 1 and Mill 12.*

Element [wt% dry mass]	SII	SV	FI
Spectrum 1			
K	11.4	30.0	10.2
Na	19.2	9.4	25.5
C	11.5	2.7	5.9
O	37.3	40	41.7
S	20.0	17.6	13.2
Cl	0.6	0.3	3.6
Spectrum			
K	23.3	28.8	20.5
Na	14.4	11.1	17.0
C	3.7	3.3	5.6
O	42.1	38.4	38.4
S	16.1	17.9	15.8
Cl	0.4	0.4	2.9
Spectrum			
K	30.5	20.8	14.6
Na	9.0	17.2	23.5
C	9.2	3.7	5.7
O	32.3	40.4	36.0
S	18.6	16.8	12.9

(Continued on next page)

Table A.3 – continued from previous page

Element [wt% dry mass]	SII	SV	FI
Cl	0.4	1.2	7.4
Spectrum			
K	19.3	30.4	28.1
Na	15.6	10.2	12.1
C	4.3	1.3	3.2
O	46.6	39.2	37.1
S	13.9	18.6	18.9
Cl	0.3	0.3	0.6
Spectrum			
K	—	30.2	9.3
Na	—	9.2	25.9
C	—	2.1	8.8
O	—	40.4	35.3
S	—	17.9	9.0
Cl	—	0.2	11.7

Table A.4: *All spectra for obtained crystals in experiment using bleed stream from Mill 2.*

Element [wt% dry mass]	1.7, 32 °C	1.7, 25 °C	1.7, 15 °C	1.9	1.10
Spectrum					
K	30.7	41.3	24.9	29.3	35.9
Na	7.6	6.4	11.7	10.9	9.1
C	6.6	0	2.9	0	0
O	37.4	29.1	43.8	46	33.1
S	17.6	23.3	16	16.8	21.9
Cl	0	0	0	0	0
Spectrum					
K	2.4	38.8	39.3	15.1	32
Na	29.5	7.3	6.8	22.5	9.9
C	7.5	0	0	4.9	0
O	39.6	31.7	31.6	37.3	38.2
S	16.8	22.2	22.3	14	19.9
Cl	4.2	0	0	6.1	0
Spectrum					
K	32.4	30.7	33.8	32.8	3.3
Na	8.9	10	10.5	9.7	29.3
C	0	0	0	0	6.3
O	39.1	40.3	34.8	36.3	40.2

(Continued on next page)

Table A.4 – continued from previous page

Element [wt% dry mass]	1.7, 15 °C	1.7, 25 °C	1.7, 32 °C	1.9	1.10
S	19.1	19	15.8	19.8	18.3
Cl	0.5	0	5	1.4	2.7
Spectrum					
K	35.3	12.6	39.6	27.9	—
Na	7.9	22.9	6.6	10.3	—
C	0	5.7	0	0	—
O	36.4	43.4	31.5	43.9	—
S	20.4	13.8	22.2	17.3	—
Cl	0	1.6	0	0.5	—
Spectrum					
K	—	31.6	33.3	—	—
Na	—	9.1	10.5	—	—
C	—	0	0	—	—
O	—	40.0	34.9	—	—
S	—	19.4	19	—	—
Cl	—	0	2.2	—	—
Spectrum					
K	—	6.2	13.5	—	—
Na	—	24.6	13.5	—	—
C	—	0	0	—	—
O	—	40.8	40.5	—	—
S	—	28.5	32.5	—	—
Cl	—	0	0	—	—
Spectrum					
K	—	1.1	—	—	—
Na	—	36.4	—	—	—
C	—	0	—	—	—
O	—	44.4	—	—	—
S	—	18.1	—	—	—
Cl	—	0	—	—	—
Spectrum					
K	—	33.5	—	—	—
Na	—	10.8	—	—	—
C	—	0	—	—	—
O	—	38.1	—	—	—
S	—	15.9	—	—	—
Cl	—	1.7	—	—	—
Spectrum					
K	—	3.3	—	—	—
Na	—	29.6	—	—	—

(Continued on next page)

Table A.4 – continued from previous page

Element [wt% dry mass]	1.7, 15 °C	1.7, 25 °C	1.7, 32 °C	1.9	1.10
C	—	6.8	—	—	—
O	—	42.3	—	—	—
S	—	14.3	—	—	—
Cl	—	2	—	—	—

A.4 Step 1: Results from Liquid Analysis

This section presents the liquid analysis for the first step of the experimental phase. Tables A.5 and A.6 shows the ICP-AES results from analysis of ML1 for Mill 1 and Mill 2, respectively.

Table A.5: *Elemental composition for ML1 from experiments performed with bleed from Mill 1.*

ML1 run	K [wt%]	Na [wt%]	SO_4 [wt%]
1.1	2.50	8.60	16.06
1.2 (2^{nd} filtration)	2.7	8.1	14.42
1.2 (3^{rd} filtration)	3.9	5.9	9.81
1.3	3.31	6.76	9.07
1.4	2.9	9.0	13.93
1.5	3.33	6.71	9.35

Table A.6: *Elemental composition for ML1 from experiments performed with bleed from Mill 2.*

ML1 run	K [wt%]	Na [wt%]	SO_4 [wt%]
1.7, 15 °C	3.12	9.56	8.37
1.7, 25 °C	2.95	8.13	7.78
1.7, 32 °C	3.08	8.12	7.98
1.9	3.13	9.16	8.10
1.10	3.17	9.18	8.47

A.5 Step 1: Calculations of maximum recovery of crystals

Run 1.7 was the first experiment where Product A was successfully crystallized. In that experiment crystals were recovered at three different temperatures: 32 °C,

25 °C and 15 °C. Results that are relevant for these calculations can be seen in Table A.7. Calculations were made to identify the temperature that yielded the maximum recovery of crystals for consecutive runs. These calculations were made before receiving analysis results. The recovery of crystals at a certain temperature, $Y_{recovery,x}$, was calculated in amount of dry crystals, in g, per extracted ML, in g. These calculations are shown in equations (A.1)-(A.3).

Table A.7: Results from run 1.7, used for calculations.

Temperature [°C]	**Crystals [g]**	**DS crystals [%]**	**ML [g]**
32	24.55	85.6	215.53
25	43.79	85.8	385
15	146	95.7	5593

$$Y_{\text{recovered},32} = \frac{24.55 \times 85.6}{24.55 + 215.53} \times 100\% = 8.75\% \tag{A.1}$$

$$Y_{\text{recovered},25} = \frac{43.79 \times 85.8}{43.79 + 385} \times 100\% = 8.76\% \tag{A.2}$$

$$Y_{\text{recovered},15} = \frac{146 \times 95.7}{146 + 5593} \times 100\% = 2.43\% \tag{A.3}$$

B

Appendix

This appendix presents information about the second step of the experimental phase of the project; re-crystallization of Product B.

B.1 Step 2: Detailed experimental measurements

Table B.1 presents detailed information about the experiments in the second step regarding masses and DS for the bleed stream, ML2 and obtained crystals. It also presents the dry mass for each component. The table includes experiments made with Product A from Mill 1 and Mill 2. Run 2.1 is not included as it was the experiment where all three saturated liquids were prepared, these can be seen in Table B.2.

Table B.1: *Detailed experimental measurements and results for experimental runs of the second step. DS is an average for the crystals.*

Run	Mass [g]	DS [%]	Mass [g, dry]
2.2			
Sat. KCl	178.4	15.5	27.6
Product A	21.7	92.3	20.0
ML2	189.5	23.3	44.1
Product B*	18.5	97.0	17.9
Run 2.3			
ML2 mimic	142.7	15.7	22.4
H_2O	35.7	—	—
Product A	21.8	92.3	20.1
ML2	201.0	14.1	28.3
Product B*	11.5	94.7	10.9
2.4			
Sat. KCl	89.2	15.5	13.8
ML2 mimic	89.2	15.7	14.0
Product A	21.7	92.3	20.0
ML2	181.1	14.8	26.8

(Continued on next page)

Table B.1 – continued from previous page

Run	Mass [g]	DS [%]	Mass [g, dry]
Product B*	19.3	97.7	18.9
Powder	6.8	97.6	6.6
2.5			
Sat. KCl	53.5	15.5	8.3
ML2 mimic	89.2	15.7	14.0
H_2O	35.7	—	—
Product A	21.7	92.3	20.1
ML2	183.9	13.7	25.2
Product B*	14.0	95.8	13.4
Powder	3.5	95.4	3.4
2.6			
ML2 mimic	160.5	15.7	25.2
H_2O	17.8	—	—
Product A	21.7	92.3	20.0
ML2	195.0	5.9	11.5
Product B*	15.1	95.4	14.4
2.7			
ML2 mimic	124.8	15.7	19.6
H_2O	53.5	—	—
Product A	21.7	92.3	20.0
ML2	200.2	14.5	29.0
Product B*	8.5	96.2	8.2
2.8			
Sat. KCl	176.2	15.5	27.3
Product A	23.8	95.7	22.8
ML2	196.0	21.6	42.3
Product B*	20.4	94.6	19.3
2.9			
ML2 mimic	141.0	15.3	21.6
H_2O	35.2	—	—
Product A	23.9	95.7	22.9
ML2	189.0	14.5	27.4
Product B*	14.6	95.1	13.9
2.10			
Sat. KCl	88.1	15.5	13.7
ML2 mimic	88.1	15.3	13.5
Product A	23.9	95.7	22.8
ML2	176.1	16.3	28.7
Product B*	25.5	93.9	23.9
2.11			

(Continued on next page)

Table B.1 – continued from previous page

Run	Mass [g]	DS [%]	Mass [g, dry]
Sat. KCl	52.8	15.5	8.2
ML2 mimic	88.1	15.3	13.5
H_2O	35.2	—	—
Product A	23.9	95.7	22.9
ML2	184.0	14.9	27.4
Product B*	20.0	90.3	18.1
2.12			
ML2 mimic	158.6	15.3	24.3
H_2O	17.7	—	—
Product A	23.9	95.7	22.8
ML2	186.0	13.9	25.9
Product B*	17.5	94.8	16.6
2.13			
ML2 mimic	123.3	15.3	18.9
H_2O	52.9	—	—
Product A	24.0	95.7	23.0
ML2	190.8	14.3	27.3
Product B*	12.3	92.2	11.3

*The product was not entirely pure Product B.

Table B.2: *Measured amounts of water and added compound to produce saturated solutions. The solutions containing Product A were prepared to mimic ML2.*

Solution	Water [g]	Added compound [g]	DS [%]
Sat. KCl	216	615	15.5
Sat. Product A Mill 1	709	160	15.7
Sat. Product A Mill 2	708	177.9	15.3

B.2 Step 2: Results from Solid Analysis

This section presents all spectra from the SEM-EDX analysis of obtained products through the screening test in the second step. Table B.3 provides the spectra from the analysis of the crystals obtained with Product A from Mill 1, while Table B.4 provides the spectra from the analysis of the crystals obtained with Product A from Mill 2.

Table B.3: *All spectra for the product obtained after the screening test using Product A from Mill 1. Index P denotes the powder that precipitated during the run.*

Element [wt% dry mass]	**2.2**	**2.3**	**2.4**	**2.4$_P$**	**2.5**	**2.5$_P$**	**2.6**	**2.7**
Spectrum								
K	44.1	6.0	35.5	41.1	36.6	45.8	13.0	27.7
Na	1.67	26.6	8.7	0.1	6.6	0.1	22.3	11.3
C	0	2.5	0.3	0	1.5	0.3	1.8	3.3
O	34.3	43.8	33.2	41.2	34.7	19.1	44	37.9
S	18.3	20.9	22.2	17.5	20.4	19.1	18.5	19.7
Cl	1.7	0.2	0.1	0.1	0.2	0.1	0.4	0
Spectrum								
K	41.9	8.0	32.9	53.8	34.1	47.1	24.2	23.6
Na	2.1	23.2	9.4	0.1	5.9	0	13.5	13.1
C	0	4.6	0.3	4.4	6.7	0.3	2.3	4.3
O	36.4	42.4	36.4	20.8	33.9	33.2	40.6	40.8
S	18.1	21.8	21.0	20.8	19.0	19.4	19.3	18.1
Cl	1.4	0.1	0	0	0.4	0.1	0.1	0
Spectrum								
K	34.1	28.9	39.3	46.5	38.7	42.9	32.3	28.4
Na	7.9	9.4	7.4	0.1	5.6	0.1	9.9	9.7
C	2.3	5.2	0.1	1.1	3.8	0.4	2.2	2.3
O	34.9	38.1	29.8	32.9	30.5	38.6	35.2	41.3
S	20.1	18.1	23.4	19.2	20.7	18.1	20.5	18.1
Cl	0.8	0.2	0	0.1	0.8	0	0	0
Spectrum								
K	24.9	14.5	49.3	43.9	45.6	43.6	15.6	30.5
Na	9.0	13.0	0.4	0.2	0.2	0	14.7	7.8
C	8.6	20.5	1.7	0.6	1.0	0.6	15.0	7.8
O	41.2	37.8	28.8	36.9	34.7	37.6	36.1	40.9
S	15.3	14.0	18.8	18.3	18.3	18.1	18.5	18
Cl	1.0	0.2	1.0	0.1	0.2	0.1	0.1	0
Spectrum								
K	37.1	—	50.3	47.8	45.4	44.5	38.7	19.3
Na	7.6	—	0.3	0.1	0.7	0.1	6.1	15.7
C	0	—	1.3	1.3	0.7	2.8	1.0	3.8
O	34.1	—	28.7	31.2	34.3	34.1	33.6	43.1
S	21.2	—	19.0	19.3	18.2	18.6	20.5	18
Cl	0	—	0.5	0.3	0.7	0	0.1	0.1

(Continued on next page)

Table B.3 – continued from previous page

Element [wt% dry mass]	2.2	2.3	2.4	2.4_P	2.5	2.5_P	2.6	2.7
Spectrum								
K	30.5	—	45.5	—	44.9	44.1	—	—
Na	10.9	—	0.4	—	0.5	0.1	—	—
C	0	—	1.3	—	0.3	0.5	—	—
O	33.5	—	34.2	—	35.4	36.9	—	—
S	16.3	—	17.9	—	18.2	18.3	—	—
Cl	8.8	—	0.7	—	0.7	0.1	—	—

Table B.4: *All spectra for the product obtained after the screening test using Product A from Mill 2.*

Element [wt% dry mass]	2.8	2.9	2.10	2.11	2.12	2.13
Spectrum						
K	42.8	29.7	53.3	43.1	33.4	43.9
Na	1.2	7.9	0.2	1.2	7.6	5.2
C	0	1.2	0.5	1.0	1.0	0
O	35.1	43.9	25.1	35.5	38.7	27.8
S	16.3	17.2	20.5	17.6	19.2	23.1
Cl	4.6	0	0.5	1.6	0.1	0
Spectrum						
K	42	32.3	48.5	43.9	24.9	35.6
Na	1.9	9.1	1.8	1.1	13.5	7.0
C	0	4.1	0.3	0.5	1.2	0
O	33.2	34.2	26.8	35.4	40.6	37.8
S	15.2	20.3	18.7	18.2	19.6	19.7
Cl	7.6	0	4.0	0.8	0.2	0
Spectrum						
K	42.1	34.5	46.8	45.4	30.0	35.1
Na	0.9	8.5	0.2	0.3	10.8	7.7
C	0	1.3	0.6	1.0	0.7	0
O	37.1	34.7	32.8	34.3	39.0	37.4
S	17.2	20.3	19.4	18.8	19.5	19.8
Cl	2.6	0	0.3	0.2	0.1	0
Spectrum						
K	44.3	14.7	44.5	42.0	17.1	34.4
Na	1.2	21.4	0.5	0.6	19.0	7.5
C	0	1.1	0.3	0.4	1.2	0
O	31.8	42.0	35.3	38.7	41.3	38.5

(Continued on next page)

Table B.4 – continued from previous page

Element [wt% dry mass]	**2.8**	**2.9**	**2.10**	**2.11**	**2.12**	**2.13**
S	16.8	20.7	18.4	18.0	21.1	19.6
Cl	5.9	0.1	1.1	0.3	0.2	0
Spectrum						
K	44.6	32.4	51.4	44.1	32.2	32.8
Na	0	6.9	0.1	0.5	8.4	8.1
C	0	4.3	0.4	1.4	4.4	0
O	32.5	39.4	27.5	35.5	35.5	40.3
S	16.6	16.8	20.5	18.3	19.5	18.8
Cl	6.3	0.1	0.1	0.2	0.1	0
Spectrum						
K	51.7	29.6	—	—	—	32.4
Na	0	9.0	–	—	—	8.2
C	0	0.6	—	—	—	0
O	28	41.9	—	—	—	40.5
S	18.4	17.8	—	—	—	18.9
Cl	1.9	0.1	—	—	—	0
Spectrum						
K	—	—	—	—	—	25.9
Na	—	—	—	—	—	12.5
C	—	—	—	—	—	0
O	—	—	—	—	—	43.5
S	—	—	—	—	—	18.1
Cl	—	—	—	—	—	0
Spectrum						
K	—	—	—	—	—	30.7
Na	—	—	—	—	—	9.5
C	—	—	—	—	—	0
O	—	—	—	—	—	40.8
S	—	—	—	—	—	19.0
Cl	—	—	—	—	—	0
Spectrum						
K	—	—	—	—	—	33.9
Na	—	—	—	—	—	7.4
C	—	—	—	—	—	0
O	—	—	—	—	—	39.2
S	—	—	—	—	—	19.4
Cl	—	—	—	—	—	0

B.3 Step 2: Results from Liquid Analysis

This section presents the liquid analysis for the second step of the experimental phase. Tables B.5 and B.6 present the ICP-AES results from analysis of ML1 for Mill 1 and Mill 2, respectively.

Table B.5: *Elemental content of the leaching solutions and ML2 for run 2.2 to 2.7.*

Element [g]	**2.2**		**2.3**		**2.4**	
	Leaching solution	**ML2**	**Leaching solution**	**ML2**	**Leaching solution**	**ML2**
K	2211.54	2311.29	714.04	924.60	1551.76	1171.46
Na	1.35	46.79	246.06	317.58	154.39	204.60
SO_4	2.36	117.47	1399.34	1812.20	875.34	452.31
Element [g]	**2.5**		**2.6**		**2.7**	
	Leaching solution	**ML2**	**Leaching solution**	**ML2**	**Leaching solution**	**ML2**
K	1109.73	965.46	802.90	883.35	624.62	904.90
Na	154.17	248.26	276.69	310.05	215.25	326.33
SO_4	875.16	864.81	1573.49	1746.42	1224.12	1804.99

Table B.6: *Elemental content of the leaching solutions and ML2 for run 2.8 to 2.13.*

Element [g]	**2.8**		**2.9**		**2.10**	
	Leaching solution	**ML2**	**Leaching solution**	**ML2**	**Leaching solution**	**ML2**
K	2184.26	1999.00	664.16	824.04	1507.79	1065.22
Na	1.34	163.84	281.20	353.43	176.47	338.05
SO_4	2.33	142.06	1315.55	1653.06	823.63	595.95
Element [g]	**2.11**		**2.12**		**2.13**	
	Leaching solution	**ML2**	**Leaching solution**	**ML2**	**Leaching solution**	**ML2**
K	1070.30	930.89	747.09	792.36	581.18	841.43
Na	176.14	334.83	316.31	355.26	246.06	352.98
SO_4	822.88	969.85	1479.81	1615.68	1151.18	1685.95

B.4 Step 2: Calculations of potassium to crystals

This section presents the calculations of the potassium that originated from the leaching solution and re-crystallized in the screening test for Mill 1 and Mill 2. The data used are presented in Tables 4.13 and 4.16. The calculations were conducted according to equation (B.1). The mass of Product A was calculated as dry.

$$K_{\text{to crystal}} = \frac{K_{\text{in leaching solution}} - K_{\text{in ML2}}}{\text{Product A}} \tag{B.1}$$

C
Appendix

This appendix provides the MATLAB code used for the evaluation of energy demand for the first step in the experimental phase and the calculations for the energy evaluation. The construction of the code is described in Section 3.3. Section C.2 offer calculations made to adjust the energy demand in terms of kJ/(g dry Product B_{dirty}).

C.1 MATLAB Code for Energy Demand Estimation

The MATLAB code processes given values of parameters that are set, and variables that are provided from Excel files. These Excel files contain all logged temperatures from the experiments and will not be disclosed in this report due to confidentiality. The script used for the fast cooling scenario is shown in Listing C.1. For the slow cooling case, the only modification was a change in the volumetric flow rate, which was adjusted to 2.5 l/min.

```
% Energy demand for run 1.1
clc;
clf;
clear;

% Known parameters
Cp_j = 3.64891492*10^3;                 % Specific heat capacity (J
    /(kg   C))
vol_rate_j = 11/60;                     % Volumetric flow rate (l/s
    )
rho_j = 1065.30208/1000;                % Density (kg/l)
mass_rate_j = vol_rate_j*rho_j;         % Mass flow rate (kg/s)

% Time setup
time_step = 60;                         % Time step (s)
total_time = 2160;                      % Total time (s)
time = 0:time_step:total_time;
num_steps = length(time);

% Load Excel data
filename = 'kodtest.xlsx';
T_jinlet = xlsread(filename, 'AB3:AB39');
T_joulet = xlsread(filename, 'AA3:AA39');
T_reactor = xlsread(filename, 'Z3:Z39');
```

```
23
24 T_jinlet = T_jinlet(1:num_steps)';
25 T_joulet = T_joulet(1:num_steps)';
26 T_reactor = T_reactor(1:num_steps)';
27
28 cooling_duty = zeros(1, num_steps);
29 for i = 1:num_steps
30     delta_T_j = T_joulet(i) - T_jinlet(i);
31     cooling_duty(i) = mass_rate_j * Cp_j * delta_T_j; % Cooling
       duty (W)
32 end
33
34 Q_cooling = trapz(time, cooling_duty); %Total energy removed (J)
35
36 % Plotting
37 fig = figure;
38 subplot(3,1,1);
39 plot(time, T_reactor, 'LineWidth', 2);
40 xlabel('Time [s]');
41 ylabel('Temperature [ C ]');
42 title('T_{reactor} over time');
43 grid on;
44
45 subplot(3,1,2);
46 plot(time, cooling_duty, 'LineWidth', 2, 'Color', [0 0.5 0]);
47 xlabel('Time [s]');
48 ylabel('Cooling demand [W]');
49 title('Cooling demand over time');
50 grid on;
51
52 set(findall(gcf, '-property', 'FontName'), 'FontName', 'Times New
   Roman');
53 set(findall(gcf, '-property', 'FontSize'), 'FontSize', 12);
54
55 disp(['Total energy consumed: ', num2str(Q_cooling/1000), ' kJ']);
```

Listing C.1: *Energy demand calculation for run 1.1 in MATLAB.*

C.2 Calculations for Conversion and Energy Demand Estimation

Table C.1 provides data that was used to calculate the approximate conversion, X, of Product A to Product B. The conversion for run 2.4 and 2.12 was calculated according to equation (C.1) and (C.4) respectively. This conversion will evidently depend a lot on the leaching solution. The conversion was calculated to 89.5 % and 72.6 %. These were further used to re-calculate the energy required for cooling, $Q_{cooling}$, for run 1.9 and 1.10. This can be seen in equation (C.2) to (C.6).

Table C.1: *Results from run 2.4 and 2.12, used for the calculations.*

Run	Product A [g, dry]	Product B [g, dry]
2.4	20.01	18.89
2.12	22.82	16.58

$$X_{2.4} = \frac{18.89}{20.01} \times 100\% = 89.5\% \tag{C.1}$$

$$Q_{\text{cooling,1.9,2.4}} = \frac{5.84}{0.895} = 6.45 \text{ kJ/(g dry Product B}_{dirty}) \tag{C.2}$$

$$Q_{\text{cooling,1.10,2.4}} = \frac{10.39}{0.895} = 11.48 \text{ kJ/(g Product B}_{dirty}) \tag{C.3}$$

$$X_{2.12} = \frac{16.58}{22.82} \times 100\% = 72.6\% \tag{C.4}$$

$$Q_{\text{cooling,1.9,2.12}} = \frac{5.84}{0.726} = 8.04 \text{ kJ/(g dry Product B}_{dirty}) \tag{C.5}$$

$$Q_{\text{cooling,1.10,2.12}} = \frac{10.39}{0.726} = 14.31 \text{ kJ/(g Product B}_{dirty}) \tag{C.6}$$

DEPARTMENT OF CHEMISTRY AND CHEMICAL ENGINEERING
CHALMERS UNIVERSITY OF TECHNOLOGY
Gothenburg, Sweden
www.chalmers.se

CHALMERS
UNIVERSITY OF TECHNOLOGY